

# Studies of the flickering in cataclysmic variables<sup>\*</sup>

## IV. Wavelet transforms of flickering light curves

Thomas Fritz<sup>1,2</sup> and Albert Bruch<sup>1,3</sup>

<sup>1</sup> Astronomisches Institut, Westfälische Wilhelms-Universität, Wilhelm-Klemm-Str. 10, D-48149 Münster, Germany

<sup>2</sup> Radioastronomisches Institut der Universität Bonn, Auf dem Hügel 71, D-53121 Bonn, Germany

<sup>3</sup> Laboratório Nacional de Astrofísica, C.P. 21, 37500-000 Itajubá, MG, Brazil

Received 4 August 1997 / Accepted 10 December 1997

**Abstract.** Wavelet transforms of a large quantity of light curves of numerous CVs in different photometric states were performed in order to quantify the behaviour of the flickering in a statistically significant sample of systems. The scalegram is used as the appropriate tool to describe the wavelet coefficients of stochastically variable data as a function of the time scale. The (logarithmic) scalegram being largely linear for all light curves shows that flickering is a self-similar process and permits a parametrization in terms of its inclination  $\alpha$  and its value  $\Sigma$  (flickering strength) at a reference time scale. For a given system,  $\alpha$  and  $\Sigma$  are stable over many years but can vary over shorter periods and are then loosely correlated. On average flickering on short time scales is somewhat bluer than on longer scales. CVs of different types (and photometric states) occupy distinct regions in the  $\alpha - \Sigma$ -plane. This behaviour is particularly clear cut for novalike variables where UX UMa stars overlap only slightly with VY Scl stars, and magnetic CVs populate a small range well separated from the other systems. The intrinsic flickering amplitudes of most dwarf novae vary around the outburst cycle with the square root of the system brightness. In dwarf novae with a strong orbital hump the inclination of the scalegram steepens during the outburst. Due probably to complex functional dependences between observable quantities, the physical origins of the flickering, and dynamical system parameters, no clear correlation (only some trends) between flickering characteristics and dynamical or geometrical properties of the CVs can be seen.<sup>1</sup>

**Key words:** binaries: close – novae, cataclysmic variables – methods: data analysis

*Send offprint requests to:* Albert Bruch

<sup>\*</sup> Based in part on observations obtained at the LNA/CNPq, Itajubá, Brazil, at the Florence and George Wise Observatory, Israel and at the European Southern Observatory, Chile

<sup>1</sup> Table 1 is only available in electronic form at the CDS via anonymous ftp to cdsarc.u-strasbg.fr (130.79.128.5) or via <http://cdsweb.u-strasbg.fr/Abstract.html>

### 1. Introduction

Cataclysmic variables (CVs) are interacting binary systems where a late type star (normally on or close to the main sequence) transfers mass onto a white dwarf. As long as the magnetic field of the latter is weak the transferred matter first forms an accretion disk out of which it is gradually accreted onto the central object. In the presence of strong magnetic fields the inner accretion disk may be disrupted (intermediate polars) or its formation may be inhibited altogether (polars) and the matter is funnelled directly to the magnetic poles of the white dwarf. For a comprehensive discussion of all aspects of CVs, see the monograph of Warner (1995).

CVs of all types exhibit stochastic brightness variations on time scales from dozens of minutes down to less than a second which can reach considerable amplitudes (up to more than a magnitude in extreme cases). This phenomenon, called flickering, manifests itself as a continuous series of overlapping flares in the light curves of CVs. It appears to be intimately related to the accretion process itself, similar phenomena occurring (on different time scales) also in other types of accreting systems (Bruch 1995).

Since flickering can reach such a high amplitude (a few tenths of a magnitude are normal) it is immediately obvious that the underlying light source contributes an appreciable fraction of the total luminosity of the systems. Therefore, we cannot claim to really understand CVs as long as the origin of the flickering remains unknown.

No physical model for the mechanism(s) leading to flickering has yet been elaborated. The first systematic study of its properties was performed by Bruch (1992; part I of this series) who gives also a review and a comprehensive list of references concerning earlier statements about flickering in the literature. He argued that for energetical reasons the main contribution to the flickering can only come from regions close to the white dwarf (inner accretion disk, boundary layer, the surface of the white dwarf itself) since sufficient (gravitational) energy is available only there to power the considerable luminosity in-

herent in the flickering. Although he did not try to construct a physical model, he envisaged turbulences in the inner disk or the boundary layer to lead to an unsteady release of gravitational energy and thus to flickering. This picture is supported by attempts to locate the site of the flickering light source. Horne & Stiening (1985) investigated RW Tri, Welsh & Wood (1995) and Welsh et al. (1996) HT Cas, Horne et al. (1994) OY Car, and Bruch (1996a,b) Z Cha. All agree that flickering in the respective systems arises in the immediate vicinity of the white dwarf. Additionally, Bruch (1996a) could show that at least in Z Cha the hot spot is another (minor) source of flickering, but only during quiescence. This supports older ideas of Warner & Nather (1971) who make an inhomogenous mass flow from the secondary responsible for the flickering.

Although some progress in understanding flickering has been achieved in recent years, its exact physical nature remains obscure. One possible way suggested by Bruch (1991) to improve the situation is to quantify observable properties of the flickering, and to look for common characteristics or differences as a function of the CV subtype and the photometric state. His database was then much too small for this purpose. However, in the meantime this has changed drastically, and enough light curves are available now to undertake a corresponding attempt.

Here, we concentrate on a study of the strength of the flickering (relative to the mean system light) as a function of the time scales at which it occurs in numerous light curves of many CVs and different photometric states. We thus address questions such as: What is the contribution of the flickering light source to the total light? To which degree do the amplitudes decrease on going from slow flares (long time scales) to rapid flares (short time scales)? To which degree are these properties characteristic for CV subtypes (dwarf novae, novalike variables, novae, magnetic systems) and photometric states (outbursts, quiescence)? Do these properties correlate with dynamical or geometrical system parameters? By answering such questions we will try to set boundary conditions for any physical model of the flickering. However, it is not the purpose of this study to develop such a model.

In order to be able to extract the information about the strength of the flickering on different time scales from light curves with stochastically overlapping flares we apply the recently developed technique of wavelet transforms (WT). This has some important advantages compared to the traditional technique of Fourier transforms, since the base functions can be chosen to resemble individual events (flares) in the light curves which are not sinusoidal in shape (Fourier transforms would then be more appropriate) but rather triangular with a largely linear rise and decline.

Since wavelet techniques are not yet widely known we give a very brief introduction into the basic theory of the WT in Sect. 3 after having presented the data base used in this study in Sect. 2. The special points to be considered in applying the WT to flickering light curves are discussed in Sect. 4. Our results are then presented in Sect. 5, and finally this work terminates with a short summary of our conclusions in Sect. 6.

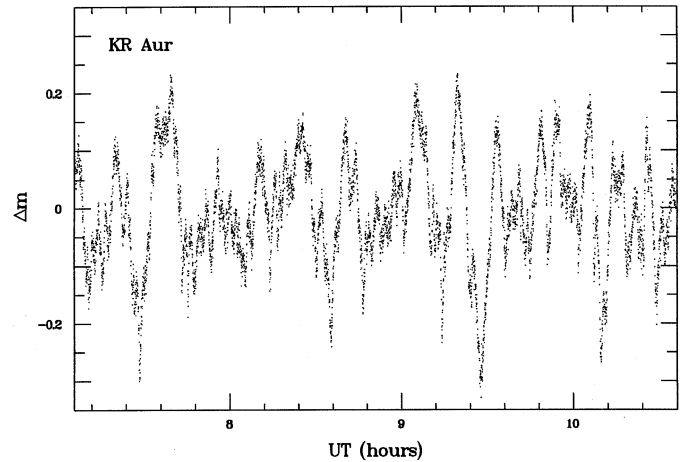


**Fig. 1.** Light curve of the novalike variable KR Aur of 1977, Nov. 14, as a typical example for flickering. The data were obtained in unfiltered (white) light; the zeropoint of the magnitude scale is arbitrary.

## 2. The data

The aim of this investigation is to perform wavelet transforms of flickering light curves and then to look for correlations between flickering properties and system parameters, systematic differences in different types of CVs or photometric states, and common characteristics. To do so, a large amount of data is required in order to obtain statistically sound results. Therefore, to have any hope of success, numerous flickering light curves of as many CVs of all subtypes as possible, observed in all states, must be available. As was already pointed out by Bruch (1992) observational material suited for such a study in fact exists so that new observations are not required. Uncounted light curves of CVs have been observed in the past decades which were never thoroughly investigated with respect to the properties of the flickering.

Many colleagues worldwide have generously put their light curves at our disposal. Most of the data have been used in other publications (not concerned with flickering). However, a considerable number was not published before. Together with our own observations performed at various occasions at different telescopes at ESO (La Silla, Chile), the Laboratório Nacional de Astrofísica (Pico dos Dias, Brazil) and the Wise Observatory (Israel) this material entered into a data bank consisting currently of more than 1300 light curves of 88 objects. It contains the equivalent of almost half a year of continuous observations. However, not all the light curves are suitable for the current study: Considering criteria outlined in Sect. 4.1 we are left with 776 light curves of 73 objects which were used here. A typical example is shown in Fig. 1.

Most of the observations were obtained in unfiltered (white) light. They have been corrected for background light and atmospheric extinction (using mean extinction coefficients appropriate for the observing site) but remain uncalibrated otherwise. A considerable number of light curves were observed with the Stiening photometer (described by Horne & Stiening 1985). It takes measurements simultaneously in four bands similar to

the standard *UBVR* bands. These data are also not calibrated. Finally, the sample contains a comparatively small number of light curves taken in the standard *UBV* and *UBV(RI)<sub>c</sub>* systems. As a consequence of the missing calibration for most data it is not possible to make statements about properties such as absolute values of the flux due to the flickering light source. Instead we are forced to content ourselves with relative values, normalized e.g. to the mean flux of the system.

Flickering occurring on a large range of time scales, in particular also on small ones (Elsworth & James 1986), the time resolution of the data should be as high as possible. The light curves used here were sampled in intervals from less than one second up to about 20<sup>s</sup> (with a strong peak in the distribution at 5<sup>s</sup>). The total time base of the observations is more than 20 years, but the distribution within this range is not homogeneous.

Although many high quality light curves of AE Aqr are available in our data bank, we excluded this system from the analysis because it is in many respects a very unusual CV (Bruch 1991, Beskrovnaya et al. 1996). This is particularly evident concerning its flickering behaviour which is unique in the sense that AE Aqr is the only known CV where phases of strong flickering alternate stochastically with phases practically devoid of flickering (Bruch 1991, van Paradijs et al. 1989, Bruch & Grütter 1997). This behaviour invalidates important premises necessary for the extraction of flickering properties from the wavelet transform of light curves and also suggests that the mechanism of flickering is different from that in normal systems, making any direct comparison obsolete. Another object discarded in spite of many available light curves is V Sge. It has so many properties which are not in line with those of *bona-fide* CVs that its membership to this group must be doubted (see Diaz & Steiner 1995 and references therein).

A journal of the observations used here together with the principal parameters distilled from the wavelet transform (see Sect. 4.6) are given in Table 1 (only available in electronic form from the CDS, Straßbourg). The various columns of the table have the following significance: (1) name of the system; (2) photometric type: N = classical nova, RN = recurrent nova, NL = novalike variable, UG = dwarf nova; (3) photometric subtype: A = fast nova, B = slow nova, VY = VY Scl star, UX = UX UMa star, AC = AM CVn star, SS = SS Cyg star, SU = SU UMa star, WZ = WZ Sge star, Z = Z Cam star; (4) magnetic type: blank = non-magnetic system (or unknown), DQ = DQ Her star (intermediate polar), AM = AM Her star (polar); (5) civil date of the start of the observations (UT) in year, month, day; (6) corresponding Modified Julian Date; (7) photometric state: – = unknown or normal state in those systems which do not exhibit different states (novalike variables and novae; outbursts of the latter are of course not considered), Q = quiescence, R = rise to outburst, M = outburst maximum, D = decline from outburst, O = unspecified outburst state (Q, R, M, D and O refer to dwarf novae in general), S = standstill (Z Cam stars), SM = supermaximum (SU UMa stars), H = high state, L = low state (H and L refer to VY Scl stars); (8) photometric system; here *UBVR\** refers to the Stiening system; (9) duration of the light curves in minutes; (10) time resolution of the data in seconds; (11) in the

case of multicolour systems the photometric band is indicated to which the information in the subsequent columns refer; (12) the scalegram parameter  $\Sigma$  (to be defined in Sect. 4.6) which is a measure of the strength of the flickering; (13) the scalegram parameter  $\alpha$  (see Sect. 4.6), a measure of the distribution of the flickering strength among different time scales; (14) mean magnitude during the observations, for light curves in uncalibrated systems a rough estimate from visual observations is given (see Sect. 5.3.4) if available, otherwise mean magnitudes and standard deviations corresponding to the respective photometric band are quoted.

### 3. The wavelet transform

The expansion of a function into base functions is a well-known and successful means to represent it in a form adapted to a particular question. An example is the Fourier transform which is a widely applied tool for harmonic analysis. In that case the base functions are sinusoids.

The flickering flares in CVs, however, have no sinusoidal but rather triangular shapes with a largely linear rise to maximum and a subsequent linear decay. This feature suggests immediately that a Fourier transform is not an ideal tool for the statistical description of flickering. Many Fourier coefficients are required to describe non-sinusoidal shapes. Moreover, non-periodic events – localized in time such as flickering flares – sampled discretely over a finite time base are only insufficiently described by a Fourier transform. Instead, another type of transformation using base functions with a shape intrinsically similar to that of the flares, permitting a resolution in frequency *and* time, should yield a more satisfying description. A prime candidate is a wavelet transform based on an appropriately chosen mother wavelet.

This is not the place to give a comprehensive introduction into wavelet theory. Therefore, we will subsequently only briefly touch the mathematical principles and focus on its application to flickering light curves in our particular case. For an overview over the basic theory, we refer to e.g. Jawerth & Sweldens (1993) and Chui (1992).

The WT permits the decomposition of a signal according to a localized function, the (finite) carrier of which is tied to the investigated scale. The base functions – the wavelets – emerge from a mother wavelet  $\psi$  via dilatation and translation:

$$\psi_{a,b}(t) = \frac{1}{\sqrt{a}} \psi \left( \frac{t-b}{a} \right) \quad (1)$$

where  $a$  and  $b$  are real numbers ( $a \neq 0$ ). The continuous wavelet transform of a one-dimensional function  $f$  is a two-dimensional function of the scale parameter  $a$  and the translation parameter  $b$ :

$$(\mathcal{W}_\psi f)(a, b) = \langle f, \psi_{a,b} \rangle = \int_{-\infty}^{+\infty} f(t) \psi_{a,b}^*(t) dt \quad (2)$$

The variable  $t$  may in principle be any quantity. Here, we will always identify it with time. Then, the WT describes the structure

of a signal at a given moment (determined by  $b$ ) and a given frequency (determined by  $a$ ). However, neither time nor frequency are exactly specified; only information on integral values over intervals can be obtained. The frequency resolution depends on the investigated time scale.

Since due to the projection of a one-dimensional function onto two dimensions the WT is redundant, its inverse is not uniquely defined. This can be avoided by the choice of discrete values for  $a$  and  $b$ : In this case,  $b$  should be chosen equidistant in  $t$  (stepwidth depending on  $a$ ), and  $a$  equidistant in  $\ln(1/t)$ . One possible choice is:

$$(a, b) = \left( \frac{1}{2^s}, \frac{k}{2^s} \right)$$

where  $s$  and  $k$  are integers. This enables the representation of the function  $f$  as a sum [discrete wavelet transform (DWT)]:

$$f(t) = \sum_{s,k} c_{s,k} \psi_{s,k} \quad (3)$$

with

$$c_{s,k} = \langle f, \psi_{s,k} \rangle = (\mathcal{W} f) \left( \frac{1}{2^s}, \frac{k}{2^s} \right)$$

The function  $\psi$  must fulfill some requirements. Only if its Fourier transform  $\hat{\psi}(\omega)$  conforms to the condition:

$$\int_{-\infty}^{+\infty} \frac{|\hat{\psi}(\omega)|^2}{\omega} d\omega < \infty \quad (4)$$

the norm is (approximately) conserved and the reconstruction of the function  $f$  through an inverse wavelet transform is possible. This implies that  $\hat{\psi}(0) = 0$  and the integral over  $\psi$  must vanish, meaning that  $\psi$  can only be an oscillating function. Thus the name wavelet.

One possible realization of a DWT is the multi-resolution-analysis (MRA) (Mallat 1989) which is used here. Basically, a signal is decomposed into its contributions on different time scales (levels): On a given level (i.e. a given value of the dilatation parameter  $a$ ), only the structures corresponding to that time scale are preserved and expressed in form of wavelet coefficients. By “summing up” the coefficients over all levels as a function of the dilatation parameter  $a$  the original signal can be reconstructed from the wavelet transform. One of the features of a DWT realized in this way is that the number of data points in a given set of measurements must be a power of two. Similarly, the investigated time scales (frequencies<sup>2</sup>) and the time resolutions increase by powers of two on going from a lower to a higher level (i.e. from a longer to a shorter time scale).

As a simple example a schematical “light curve” is shown in Fig. 2 (top). The lower part of the diagram shows the two-dimensional representation of the coefficients of a wavelet transform [using the Haar wavelet (Daubechies 1992) in this particular case]. The coefficient of the wavelet  $\psi_{s,k}$  contains information about the significance of a structure similar in shape to  $\psi$  at

<sup>2</sup> We understand the term “frequency” here somewhat loosely as the inverse of the time scale.

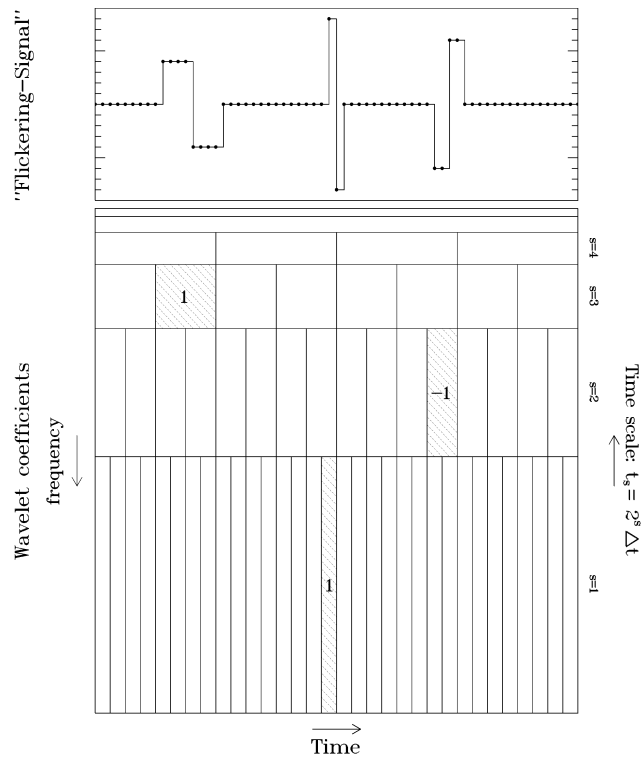


**Fig. 2.** Schematical light curve with flares and dips (top) and the two-dimensional array of the coefficients of a wavelet transform using the Haar-wavelet (bottom). The coefficients represent the light curve structures in time (depending on when they occur) and frequency (depending on their duration) in “Heisenberg-boxes”: Broad structures are not well localized in time but have a well defined frequency; narrow structures are well confined in time at the expense of a corresponding uncertainty in frequency.

a location  $2^{-s}k$  in time and at a frequency  $\sim 2^s$ . The maximum frequency is the Nyquist frequency  $1/(2 \Delta t)$  where  $\Delta t$  is the time resolution of the data. The frequency resolution depends on the parameter  $s$  of the wavelet which thus determines the (time) scale. Scale and frequency are connected to each other: a small scale corresponds to a high frequency and permits a good time resolution but a bad frequency resolution (and vice versa for large scales). In the idealized case of the “light curve” in Fig. 2 only three coefficients are different from zero (cross-hatched in the lower part of the figure). These are located in time at the locations of the corresponding structures in the signal, and correspond in frequency to the time scales on which the structures occur.

Of course, the correct choice of the mother wavelet is important. The use of the orthogonal MRA which is numerically stable, demands the choice of orthogonal wavelets and thus ensures the conservation of the norm. Moreover, the wavelet should be as compact as possible, enabling the recognition of sharp structures in the signal. On the other hand it should have a high number of vanishing momenta which ensures a good frequency localization. For the present work we have made experiments

with the following wavelets: the Haar wavelet, the Daubechies wavelets (D4 – D20), the Coiflets (C6 – C30), and a few others which proved to be of no importance for our application. For a detailed description of the properties of these wavelets, see Daubechies (1992).

#### 4. Application to flickering light curves

##### 4.1. Requirements on the light curves

The light curves which are to be subjected to the wavelet transform should fulfill several requirements.

The sampling should be equidistant. This is in general the case within uninterrupted blocs of measurements. But most light curves were interrupted from time to time for sky background measurements, breaking the equidistant sampling. However, if one is not interested in the exact temporal location of particular structures in the light curve (see Sect. 4.3) short gaps can just be ignored, and an equidistant sampling may be assumed. Alternatively, a linear interpolation across such gaps is possible, recognizing that this will induce structures on time scales longer than the gap width while on shorter time scales the wavelet coefficients will vanish at the gap location.

Variations in CVs are not only due to flickering. Other sources of variability act on a large range of time scales: Superhumps in SU UMa stars in superoutbursts; orbital humps due to the hot spot as well as intermediate humps in some systems; eclipses of the primary component by the red dwarf; intermediate polar type variations; quasiperiodic and periodic oscillations in outbursting dwarf novae and in novalike variables. On all time scales to be sampled the variations which are to be investigated by the WT should only be due to flickering in the ideal case. Thus, flickering on very long time scales cannot be studied if e.g. orbital variations or superhumps are superposed. Similarly, since flickering amplitudes decrease towards short time scales, noise may mask flickering there. In eclipsing systems the eclipses interrupt the flickering signal regularly, constituting larger gaps and thus causing problems on intermediate time scales. As in the case of gaps due to background measurements they can be ignored if one is not interested in the time information. Only if largely differing data values just before and after the gap occur they may influence wavelet coefficients on short and intermediate time scales, but only locally. This is more easily tolerated than the consequences of an interpolation over large gaps which would modify the coefficients drastically on many time scales. Large amplitude periodic variations in intermediate polars occur either above the interesting time scales or only influence the coefficients on just one particular scale and are thus easily recognized. Quasiperiodic and periodic oscillations in dwarf novae and novalike variables occur on time scales which are so short that in all but the most extreme cases noise dominates. In general, they can therefore be ignored.

The light curves should be long enough because the transformation with any wavelet (with the exception of the trivial Haar wavelet) leads to errors due to edge effects. In order to treat these, the periodic WT (Press et al. 1988) is used. This is

in the present connection the appropriate algorithm to analyse flickering which occurs on time scales short compared to the total duration of the light curves. The longest time scale containing significant information is then limited to about an eighth of the light curve length, depending in detail on the choice of the wavelet. Thus, the two highest levels (longest time scales) are not trustworthy. Since the number of data points must be a power of two (see Sect. 3) we only regarded light curves containing at least  $2^8 = 256$  measurements.

All light curves were expressed as fluxes. However, since most of them were not calibrated the flux scale is in general arbitrary. This can be done because absolute values are of no importance. Only flux ratios will be regarded (see Sect. 4.3.)

##### 4.2. The choice of the optimal wavelet

The possibility to choose a base function appropriate to a given problem makes the WT superior to a Fourier transform if the signal cannot well be described by a superposition of infinite periodic functions. Events localized in time remain localized after the transformation without causing global effects. They can thus be recognized as belonging to a certain scale, while at the same time the WT requires only a minimal number of significant coefficients for its representation in the given base. Thus, with an optimal base function the WT can be very effective in recognizing corresponding structures.

To find such an optimal base a cost function is required which should be minimal if the base describes the signal efficiently with few significant coefficients. A suitable cost function is the Shannon information entropy of the wavelet coefficients (Coifman & Wickerhauser 1992):

$$I = - \sum_{s,k} p_{s,k} \ln p_{s,k} \quad (5)$$

with

$$p_{s,k} = \frac{c_{s,k}^2}{\sum_{s,k} c_{s,k}^2}$$

Here, the  $c_{s,k}$  are the wavelet coefficients and  $p_{s,k} \ln p_{s,k}$  is assumed to vanish for  $p_{s,k} = 0$ .  $I$  becomes large if many coefficients have similar values and small if the information is concentrated in few coefficients. The base function best adapted to the signal is thus the one which leads to a minimal information entropy.

The information entropy is an individual property of each light curve. In order to ensure the comparability of results from many light curves a wavelet must be found which represents flickering flares in all of them with as few (significant) coefficients as possible. We selected those 85 light curves of our sample with the highest count rates<sup>3</sup> in order to minimize at least the disturbing effect of Poisson noise. Their wavelet coefficients on intermediate scales can be considered as being largely independent of noise and edge effects. They were subjected to a WT

<sup>3</sup> We understand count rates here as the number of counts *per integration interval* which is not necessarily equal to the unit of time.

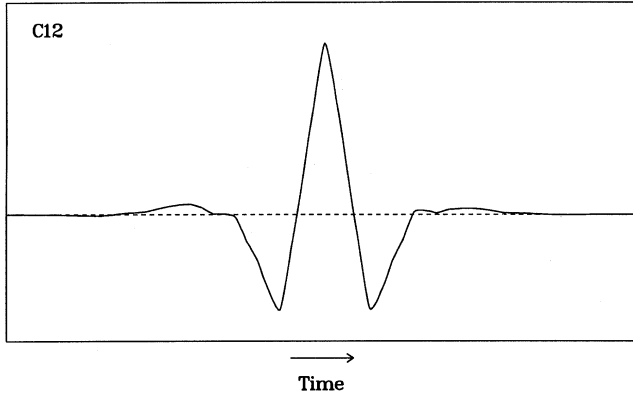


**Fig. 3.** Wavelet C12 which was found to be optimally suited for a WT of flickering light curves.

using all the wavelets named in Sect. 3, and the information entropy was calculated. An appropriate normalization (described in detail in Sect. 4.3) was performed to account for the different lengths of the light curves. In order to study the dependence of the entropy on the investigated time scales, in addition to the procedure outlined above some light curves were subjected to high and low pass filters, respectively, before the analysis. No significant differences were found which may be regarded as an indication for a uniformity of flares on different scales. Possible dependences on flare rates and amplitudes were searched in artificial flickering light curves and were not detected.

As a result it was found that the Coiflets C12, C18 and C24 can represent the flickering flares best. The Daubechies wavelets D4 and D6 also yield satisfying results, while the Haar wavelet is not appropriate. To be definite, the C12 wavelet was chosen as the optimal base function for the subsequent investigations. It is shown in Fig. 3. Its shape is indeed very reminiscent of a flickering flare, including the declining part of the previous and the rising part of the subsequent flare.

#### 4.3. The scalegram

Flickering is a stochastic process. Therefore, it is not important when exactly a particular event occurs in a light curve. Thus, the time information provided by the MRA is of no interest. However, the distribution of events among different time scales can obviously tell us something about the driving mechanism behind the process. Scargle et al. (1993) introduced the scalegram for the analysis of stochastic data. They define a measure of the variance of the wavelet coefficients on a given scale:

$$S'_s = \frac{2^s}{N} \sum_k c_{s,k}^2 \quad (6)$$

Here  $k$  is the time index,  $N$  is the number of data points in the signal, and  $s$  is the scale index which is connected to the time scale by  $t_s = 2^s \Delta t$ . The function  $S'(t_s)$  is then the scalegram, describing statistically the variations of the signal within the interval  $[2^s \Delta t, 2^{s+1} \Delta t]$ .

$c_{s,k}^2$ , multiplied by the time interval  $\Delta T$  to which it corresponds, can be regarded as the “energy” of the variable signal in the time bin  $k$  at the time scale  $t_s$ .  $\Delta T$  is given by the product of the time resolution  $\Delta t$  of the data and the number of time bins at the scale  $t_s$ :  $\Delta T = 2^s \Delta t$ . Thus,  $S'_s$  is the total energy of the signal at the time scale  $t_s$ , summed over all time bins, normalized to the total number  $N$  of wavelet coefficients (which is equal to the number of measurements) and the integration interval.

The conservation of the norm implies  $\sum_{s,k} c_{s,k}^2 = \sum_i x_i^2$ , where the  $x_i$  are the values of the data points (e.g. count rates) which will increase in proportion to  $\Delta t$  and will also depend on details of the instrumentation used during the observations. Therefore, in order to enable a comparison of the scalegrams of light curves observed under different conditions and with different time resolutions, a suitable normalization removing these effects is required. Expressing the signal energy at  $t_s$  as a function of the total energy (summed over all time scales) would be a comparable measure for all light curves. Therefore,  $S'_s$  is first multiplied by  $N \Delta t$  which gives the signal energy at  $t_s$ , and then divided by the total energy which is simply the sum over the squares of all wavelet coefficients. Thus, the energy normalized scalegram is:

$$S(t_s) = S'(t_s) \frac{N \Delta t}{\sum_{s,k} c_{s,k}^2} = S'(t_s) \frac{N \Delta t}{\sum_i x_i^2} \quad (7)$$

The last equality is due to the conservation of the norm. The normalized scalegram is a measure of the mean relative energy within the variations of the signal on different time scales. It thus describes the variance of the modulated part of the light curve in units of the mean of the square of the data points<sup>4</sup>. Since due to this normalization any scaling of the signal – affecting its variable and constant part equally – does not change the scalegram, results from uncalibrated light curves (usually only given as count rates) can be compared to each other.

While the classical power spectrum is certainly superior to the scalegram for the detection of periodic signals, the latter is better suited to study processes which extend over numerous octaves in frequency space. Relations occurring across many time scales are enhanced. Thus, the scalegram has the advantage to reveal structures similar in shape to the chosen base function on many different scales.

#### 4.4. Error estimates via bootstrap replications

Since each light curve is unique there is no way to determine objectively the errors of the scalegrams if one does not want to assume that different light curves of a given system have the same statistical properties (which is in fact one of the questions to be addressed in this study) so that mean values and standard deviations could be calculated from an ensemble of light curves. But even so it is possible to obtain satisfactory estimates of the errors by using bootstrap replications. The application of this

<sup>4</sup> Note that in all cases but those with an extremely strong flickering the approximation  $\sum_i x_i^2 / N \approx \langle x_i \rangle^2$  is valid. Thus,  $S(t_s)$  can be regarded as being normalized to the squared mean of the signal.

method to the present problem will be briefly outlined here. For an encompassing discussion, see Efron & Tibshirani (1993).

Assume an observed sample of data  $z$  to be composed of independent measurements  $z_i$  drawn from an unknown distribution  $F$ . Applying a function  $g$  to the observations yields an estimate  $\hat{\Theta}$  of the (unknown) true parameter  $\Theta$  of  $F$ . Repeating the measurements many times permits the determination of the scatter of  $\hat{\Theta}$ . However, if only one set of measurements is available, and if  $g$  is not a simple function, simulations must be used to determine the scatter and thus the errors. The bootstrap method assumes that the empirical distribution  $\hat{F}$  constructed from the  $z_i$ -values can be regarded as an approximation of the true distribution  $F$ . Another sample of (simulated) measurements  $z^*$  may then be drawn at random from the distribution  $\hat{F}$ . Subjecting it to the function  $g$  yields another estimate  $\hat{\Theta}^*$  of the parameter in question. The repeated application of this recipe leads to a sample of replications  $\hat{\Theta}^*$ , the standard deviation of which is called the bootstrap estimate of the error of  $\hat{\Theta}$ .

The bootstrap error is always an overestimate consisting of two components: The error of the original sample which depends on the number  $N$  of data points, and the error of the bootstrap samples which decreases with their number  $B$ .  $B$  is a critical parameter of the method. A sensible value depends on  $N$  and the expense to calculate  $g$ . We found  $B = 50 \dots 200$  to be sufficient for a satisfactory error estimate here.

In the present case the observed sample  $z$  is the light curve and the function  $g$  is the prescription to calculate the scalegram points which are to be identified with the parameter  $\Theta$ . Of course, points in a flickering light curve are not independent and thus one of the principal assumptions of the bootstrap method is not fulfilled. This problem is overcome by using the moving block method: The bootstrap samples are not constructed by taking individual points of the light curves, but by combining blocks of length  $L$ , chosen at random from the original light curve. If  $L$  is longer than the correlation length of the data points (to be determined easily from the auto-correlation-function of the light curves) the blocks can be regarded as independent.

The application of this method is possible here because the discontinuities in the composed light curves at the edges of the individual blocks have no serious effects on the scalegrams because they do not alter the WT globally. However, structures on long time scales are destroyed by the resampling, falsifying the wavelet replications for scales above the blocklength  $L$ . On the other hand it was mentioned above that the very long time scales are unreliable also for other reasons. Therefore,  $L$  was generally chosen to be a quarter or an eighth of the entire light curve. This is also comfortably above the correlation length of the flickering.

Fig. 4 contains the original scalegram of a light curve of the dwarf nova RX And of 1976, Aug. 21 (dots connected by a broken line) together with scalegrams of 50 bootstrap replications (points). The solid line represents the mean of the bootstrap results. It deviates significantly from the original scalegram only at long time scales, where it is unreliable anyway.

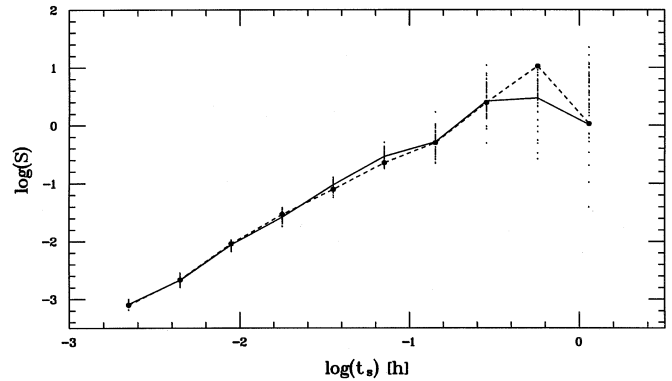


**Fig. 4.** Scalegram of the light curve of the dwarf nova RX And of 1976, Aug. 21 (large dots, connected by the broken line) and results of bootstrap replications (small dots). The solid line connects the mean values of the bootstrap replications at each time scale. Significant differences from the scalegram of the original data occur only at long time scales, where the WT is unreliable.

#### 4.5. Correction for noise and other disturbances

##### 4.5.1. Poisson noise

White noise remains white noise in an orthogonal discrete WT (Donoho 1992, Donoho & Johnstone 1993) and thus contributes to the scalegram on all scales. Since the (unnormalized) scalegram consists of the variances of the wavelet coefficients at the different scales it is easy to correct for Poisson noise if the (mean) count rates  $Z$  of the light curves are known. This yields the Poisson corrected scalegram:  $S'_{\text{pc};s} = S'_s - Z$ . But note that  $S'_{\text{pc};s}$  is not identical to  $S'_s$  of the noise-free signal because the latter does not contain contributions of coefficients on small scales which make up for noise-induced structures on larger scales.

In the (logarithmic) scalegrams of flickering light curves, noise causes a turnover on small time scales from a largely linear decline to a constant value which depends on  $Z$ . The scale at which this happens decreases with the S/N-ratio of the flickering signal.

For many of the light curves used in the present study the Poisson corrected scalegrams cannot be obtained because the original count rates are unknown. Therefore, the influence of Poisson noise on the energy normalized scalegram should be investigated. For a pure noise signal with a variance  $\sigma^2 = Z$ , the relation

$$S(t_s) = \frac{\sigma^2}{\frac{1}{N} \sum_i x_i^2} \Delta t = \frac{Z}{Z^2} \Delta t = \frac{1}{Z} \Delta t \quad (8)$$

holds.  $S$  is thus a constant for all scales. Its value is statistically most securely determined at the smallest scale since half of all wavelet coefficients contribute to  $S_1$ . We define the relative noise level  $\epsilon = \sqrt{S_1/\Delta t}$  which can be directly obtained from the scalegram. Note that no knowledge of the original count rates is required.  $\epsilon$  describes the fractional contribution of the Poisson noise to the total variance of the signal.

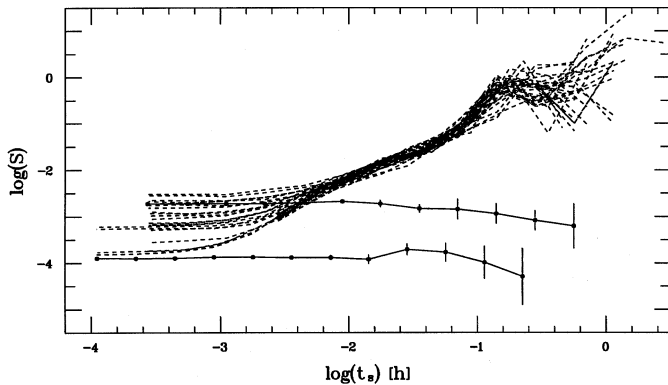


**Fig. 5.** Scalegrams of all unfiltered as well as *B* and *V* band light curves obtained in the Stiening system of the intermediate polar AO Psc (broken lines). The differences at small time scales are due to different Poisson noise contributions. The solid lines are scalegrams of Poisson noise sequences corresponding to a count rate as found in the AO Psc light curves with the highest and lowest S/N ratio, respectively.

For light curves with other variations apart from Poisson noise, it is easily seen that  $(\sum_i x_i^2)/N > Z^2$ . However, even in the presence of quite strong flickering the difference is found to be small enough to be negligible. Therefore, also in these cases  $\epsilon$  can be determined from the value of  $S_1$  if the scalegram is dominated by noise at this scale. However, the residual influence of flickering causes a systematic overestimation of the relative noise level.

Fig. 5 shows the superposed scalegrams of our light curves of AO Psc<sup>5</sup>. The turnover from the linear decline towards small scales to a constant level occurs at different time scales according to the different S/N ratios (for some light curves with a comparatively coarse time resolution this point is not reached). Additionally, the figure contains scalegrams for two Poisson noise sequences corresponding to the highest and lowest noise levels, respectively, of the real light curves. The latter lie below the flat parts of the corresponding AO Psc light curve scalegrams, indicating the presence of additional noise sources on small scales. It can be due to e.g. small scale flickering and atmospheric disturbances (but note that pure scintillation effects should be small compared to Poisson noise for the stars under study here; see the discussion in Bruch 1996a).

For those light curves for which the original count rates are available a correction of the scalegrams, i.e. a subtraction of the scalegram of the corresponding Poisson noise sequence, has been performed. Only the smallest scales are noticeably affected. While this correction can certainly not yield a noise free scalegram it shifts the turnover point to smaller scales and enables thus the study of the flickering in a broader range of time scales.

#### 4.5.2. Atmospheric disturbances

A considerable number of our light curves were observed with a two channel photometer, the second channel of which was used

<sup>5</sup> The hump at the time scale of  $\approx 15^m$  is caused by the intermediate polar type variations of this system.

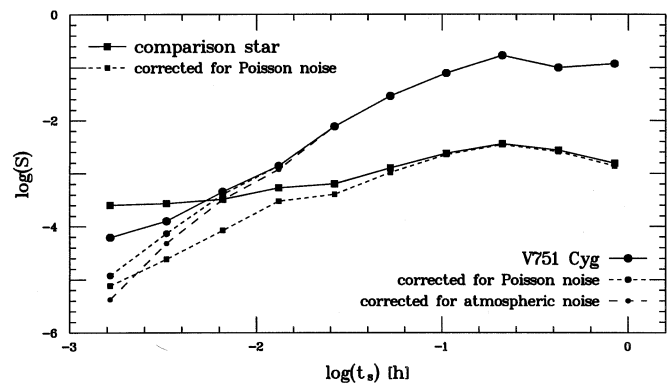


**Fig. 6.** Scalegrams of the light curve of V751 Cyg of 1977, June 20 (dots) and of a simultaneously observed constant comparison star (squares). The latter is not flat after a correction for Poisson noise. This indicates apparent variability due to atmospheric disturbances which must also be expected to modify the scalegram of V751 Cyg. A corresponding correction affects only the small time scales noticeably.

to monitor a constant comparison star close to the target star. In these cases it is possible to investigate the influence of atmospheric disturbances such as variations of the sky transparency on the scalegrams since the relative variations of the comparison star due to these effects are expected to be also present in the light curves of the variable<sup>6</sup>.

The energy normalized scalegram of a constant program star is then – after correction for Poisson noise – identical to that of the comparison star. A difference would indicate intrinsic variability of the program star, i.e. flickering in the present case. In order to correct for the atmospheric disturbances, the energy normalized, Poisson noise corrected scalegram of the comparison star C must be subtracted from that of the program star P, yielding the atmosphere corrected scalegram  $S_{ac;s}^P = S_{Pc;s}^P - S_{Pc;s}^C$ .

Fig. 6 shows the correction procedure at the example of a light curve of V751 Cyg. The observations of the comparison star showed that the atmospheric disturbances are comparatively high in this particular light curve. Thus, this is a rather extreme case. Even so the correction affects only small time scales. In view of the parametrization of the scalegram to be introduced in Sect. 4.6 it means that atmospheric disturbances have practically no bearing on the strength of the flickering at a reference time scale of  $3^m$  but can systematically (but moderately) modify the inclination of the linear part of the scalegram.

#### 4.5.3. The contribution of the secondary component

The secondary star of a cataclysmic variable can be excluded as the source of the flickering (Bruch 1989, 1996a). It is therefore sensible to relate the variations to the flux of the primary. This requires a subtraction of the contribution of the secondary to the total light. In most cases the secondary is so faint compared to the other light sources in the system that its contribution can be neglected in the visual spectral range. However, there are

<sup>6</sup> We neglect higher order effects such as e.g. a variable amount of scattered moonlight going along with sky transparency variations.

some exceptions. For these, Beckemper (1995) has estimated the relative contribution of the secondary in the  $UBVR$ -bands.

While in no case a correction is necessary in outburst states, we corrected the quiescent light curves of WW Cet, T CrB, SS Cyg, DO Dra, RS Oph, and GK Per for the mentioned effect. HT Cas has a close optical companion, permitting only to measure the combined light, and was subjected to a similar correction. In the case of white light curves it was assumed that the contribution of the secondary is the same as in  $B$  because that band is expected to have an effective wavelength similar to that of unfiltered light for blue stars such as CVs.

#### 4.6. Parametrization of the scalegram

In order to be able to compare the scalegrams of many light curves of numerous objects it is desirable to condense their essence into a few parameters, the distribution of which will then permit insight into differences and similarities of the flickering behaviour of the investigated stars as well as into the development of its properties with time or photometric state.

As mentioned in Sect. 4.1 the scalegram is unreliable on very long time scales and is dominated by noise at very short ones. Thus, the intermediate scales contain the information concerning the flickering. In this range we always found an approximately linear rise from small to long time scales (on the double logarithmic scale). This behaviour is typical for self-similar processes (Steiman-Cameron et al. 1994): A function  $x(t)$  is called self-similar with an exponent  $\beta$  if  $x(\lambda t) = \lambda^\beta x(t)$ . For a scalegram self-similarity means  $S'_s \propto s^{2\beta}$  (the factor 2 enters into the exponent because the wavelet coefficients are squared). In the logarithmic scalegram this translates into a linear relation with an inclination  $\alpha = 2\beta$ .

The interesting part of the scalegram can thus be described by the two parameters which uniquely define this linear relation: its inclination and its value at a reference time scale. The inclination  $\alpha$  is determined by a linear least squares fit to the scalegram points, weighted with their bootstrap errors. Only those points are included which are definitely above the noise level. In any case the lowest considered time scale point get less weight than the others. The point corresponding to the longest time scale in the scalegram is always disregarded, as are all points on time scales longer than one hour. In those cases where periodic variations occur on the relevant time scales, the corresponding points were disregarded or were given less weight. This refers mainly to some intermediate polars.

The second parameter is the value of the scalegram at a reference time scale:  $\Sigma = \log S(t_{\text{ref}})$ .  $t_{\text{ref}}$  must be chosen such that the scalegram at this scale is not appreciably influenced by noise or atmospheric effects, and that on the other hand enough wavelet coefficients contribute to its value, making it statistically well defined. We found the best value to be  $t_{\text{ref}} = 0^{\text{h}}05 = 3^{\text{m}}$ . In order to remain independent from slight peculiarities of the flickering in a particular light curve,  $\Sigma$  is taken from the linear fit to the scalegram, not from the scalegram values themselves.

Thus, the parameter  $\alpha$  describes the distribution of the energy of the flickering signal among the different time scales:

As long as  $\alpha > 0$  (which was found to be the case in all light curves) flickering on long time scales is stronger than on short ones. However, the smaller  $|\alpha|$  is, the more similar is the flickering strength on all time scales. To simplify the language we will talk about strong (faint) flickering on short (long) time scales if  $\alpha$  is small (and vice versa for large  $\alpha$ ), keeping in mind that on absolute terms flickering is always stronger on longer time scales than on shorter ones.

The parameter  $\Sigma$  is a measure of the intensity or the strength of the flickering on the reference time scale. More specifically, it measures the square of the flickering signal relative to the square of the mean signal (see Sect. 4.3), eventually corrected for the contribution of the secondary star (see Sect. 4.5.3). Henceforth we will refer to  $\Sigma$  simply as the flickering strength. It is important to recognize that the flickering strength defined in this way is not an unbiased measure of the flux due to the flickering light source. The latter must be expected to consist of a modulated part which is seen as flickering and an unmodulated part. There is no way to determine the degree of modulation of the flickering light source (only of that of the total light) and therefore the strength of the flickering is only a measure of a lower limit of the total flux of the flickering light source.

The two parameters  $\alpha$  and  $\Sigma$  taken together describe the scalegram behaviour uniquely (within the accuracy attainable by this parametrization). The behaviour of the flickering in a particular light curve can therefore be characterized by its location in a two-dimensional diagram, formed by the  $\alpha$ - $\Sigma$ -plane.

Of course,  $\alpha$  and  $\Sigma$  cannot represent the scalegram perfectly. There are systematic residuals between the linear fit and the real data. They can indicate small deviations from a perfect self-similarity of the flickering on a given scale, i.e. an enhancement or a deficiency of its strength. It was found that no additional useful information about the flickering could be extracted from these residuals.

## 5. Results and discussion

The WT was applied to the 776 suitable light curves of 73 objects available to us. In all cases the errors of the scalegrams were estimated via bootstrap replications. The parameters  $\Sigma$  and  $\alpha$  are listed together with their formal errors in Table 1 (only available in electronic form from the CDS, Strasbourg). In this section we will present and discuss the results. We will first concentrate on some general properties, turn our attention then to characteristics of different types of CVs, and will finally search for correlations with geometrical and dynamical system parameters.

### 5.1. The long term behaviour of the flickering

For several of the studied CVs, light curves spanning a long time (more than 20 years in the most extreme case) are available, enabling us to study the long term stability of the flickering behaviour via an investigation of the parameters  $\Sigma$  and  $\alpha$  as a function of time. However, this is only sensible if the photometric state of the system is well defined and the same for all light

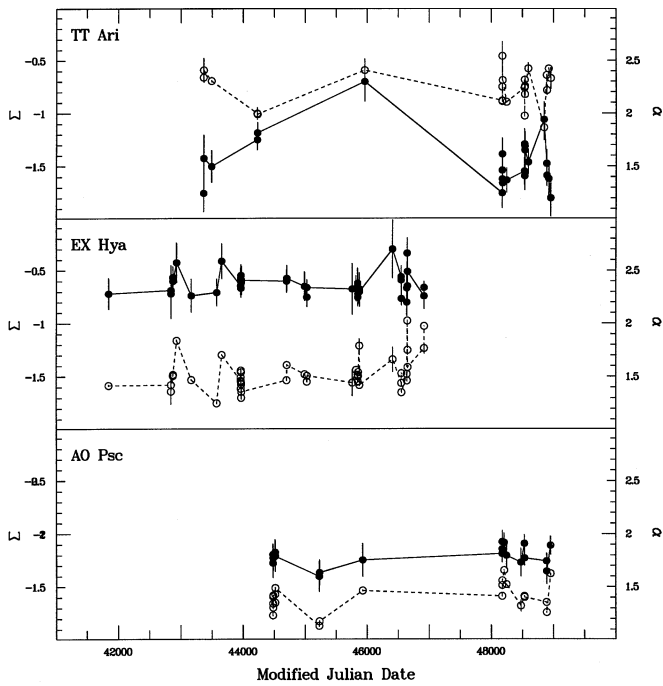


**Fig. 7.** Variations of  $\Sigma$  (left hand scale; filled dots, connected with solid lines) and  $\alpha$  (right hand scale; open dots, connected with broken lines) over a time base of several years for the three systems TT Ari, EX Hya and AO Psc. Whereas  $\Sigma$  appears to be stable within the error limits (but see text), variations of  $\alpha$  are clearly significantly larger than their error bars (which are often smaller than the plot symbols), revealing intrinsic variability.

curves. Therefore, this study is restricted to classical novae, novalike variables (in the high state in the case of VY Scl stars) and some dwarf novae during quiescence. Since the flickering properties of dwarf novae change considerably when they erupt (see Sect. 5.3.4) outburst states are not considered.

In Fig. 7  $\Sigma$  and  $\alpha$  are shown as a function of Modified Julian Date for three examples, namely the VY Scl-type novalike variable TT Ari, the dwarf nova and intermediate polar EX Hya, and the intermediate polar AO Psc. In the case of multicolour light curves, the results obtained in the  $B$ -band are given here for reasons explained in Sect. 4.5.3.

There is a certain scatter, but the variability of the parameters remains within narrow limits. The only strongly deviating point is seen in TT Ari on MJD 45962 (1984, Sep. 19) when  $\Sigma$  was considerably larger than otherwise. However, TT Ari might have been fainter than in its normal high state at this date. While no contemporaneous magnitude measurements are available to us, Verdenet (1984) found TT Ari to be in a low state around 15<sup>m</sup>:5 during December 1983, and Verdenet (1985) and Bortle (1985) observed it to emerge slowly from a low state between January and March of 1985. If TT Ari was really in a faint state in September 1984, this indicates the capacity of  $\Sigma$  as an indicator of photometric state.

The error bars at the  $\Sigma$ - and  $\alpha$ -points suggest, that the small variations are significant for  $\alpha$  within the formal errors (the error bars are often smaller than the plot symbols themselves).

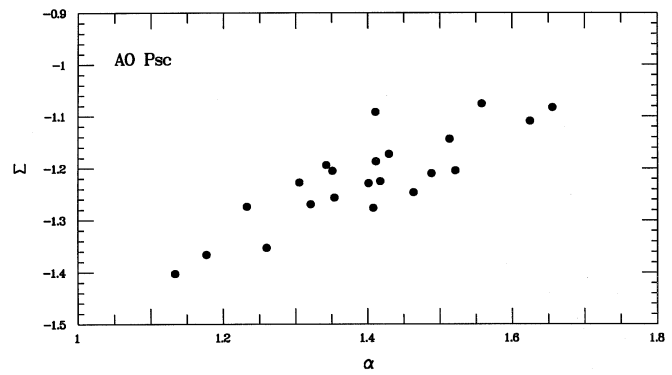


**Fig. 8.** Correlation between the scalegram parameters  $\alpha$  and  $\Sigma$  for the light curves of the intermediate polar AO Psc.

But for  $\Sigma$  this seems not to be the case. Simple statistical tests confirm indeed the significance of the  $\alpha$  variations and show that the variations found for  $\Sigma$  are compatible with accidental fluctuations.

However, there is a strong argument against the view of an intrinsically constant  $\Sigma$ : If it were really constant, it should not correlate with variations in  $\alpha$ . The results of a corresponding investigation are listed in Table 2, which apart from the name and photometric states of the systems contains the number of involved light curves, their total time base, the inclination of a linear fit to the  $\alpha - \Sigma$ -values, the correlation coefficient  $r$  between  $\alpha$  and  $\Sigma$ , and the probability  $P$  to find a value of  $|r|$  larger than actually measured if the  $\alpha$ 's and  $\Sigma$ 's were drawn accidentally from uncorrelated samples (“false alarm” probability). It is seen that for the majority of the cases a significant correlation (large  $|r|$ , small  $P$ ) exists<sup>7</sup>. The most convincing case is AO Psc which is illustrated in Fig. 8. In most systems  $\Sigma$  increases with  $\alpha$ , meaning that the distribution of the flickering strength among different time scales becomes steeper as the flickering becomes stronger, i.e. flickering on small time scales decreases. However, there are two notable counterexamples where the  $\alpha - \Sigma$ -relation is inverted, namely RR Pic (marginally significant) and TT Ari (highly significant).

## 5.2. The colour of the flickering

It is well known that the flickering light is very blue (Bruch, 1992). Beyond this general statement the present investigation permits us to say something about colours of flares occurring on different time scales. However, this is not straightforward because in most cases the multicolour light curves available here (in particular the data obtained in the Stiening system) are not calibrated and because the normalization of the scalegram permits us only to determine a measure of the fractional contribution of the flickering light to the total light. This will depend strongly on the spectrum of the constant radiation sources, i.e. basically the non-variable fraction of the accretion disk light.

<sup>7</sup> Note that in the case of VW Hyi in quiescence and supermaximum one, and for WZ Sge two data pairs, deviating strongly from the others, were disregarded.

**Table 2.** Correlation between  $\alpha$  and  $\Sigma$ 

Name	state	N	$\Delta T$ (days)	inclination $\alpha - \Sigma$	corr. coef.	$P$
TT Ari	H	22	5591	$-1.62 \pm 0.45$	-0.63	$7.3 \cdot 10^{-4}$
BG CMi	Q	14	377	$0.01 \pm 0.33$	0.01	$9.9 \cdot 10^{-1}$
HT Cas	Q	12	1558	$0.41 \pm 0.32$	0.73	$2.2 \cdot 10^{-3}$
Z Cha	Q	16	4724	$1.00 \pm 0.31$	0.65	$2.8 \cdot 10^{-2}$
Z Cha	SM	19	2127	$0.17 \pm 0.33$	0.13	$5.9 \cdot 10^{-1}$
TV Col		21	2192	$1.87 \pm 0.48$	0.67	$3.1 \cdot 10^{-4}$
U Gem	M	10	723	$1.77 \pm 0.63$	0.71	$8.5 \cdot 10^{-3}$
EX Hya	Q	38	4810	$0.94 \pm 0.26$	0.52	$4.6 \cdot 10^{-4}$
VW Hyi	Q	21	4812	$1.18 \pm 0.40$	0.56	$5.1 \cdot 10^{-3}$
VW Hyi	SM	21	4710	$0.60 \pm 0.23$	0.52	$1.1 \cdot 10^{-2}$
V2051 Oph	Q	27	2939	$1.32 \pm 0.42$	0.54	$2.3 \cdot 10^{-3}$
GK Per		14	5049	$0.09 \pm 1.39$	0.02	$9.5 \cdot 10^{-1}$
RR Pic		20	4408	$-0.60 \pm 0.25$	-0.49	$1.9 \cdot 10^{-2}$
AO Psc		22	4475	$1.28 \pm 0.18$	0.85	$1.2 \cdot 10^{-8}$
CP Pup		20	1130	$0.79 \pm 0.25$	0.60	$2.6 \cdot 10^{-3}$
WZ Sge	Q	34	1177	$1.14 \pm 0.22$	0.67	$2.7 \cdot 10^{-6}$
V1223 Sgr		21	2316	$1.24 \pm 0.37$	0.61	$1.5 \cdot 10^{-3}$
V3885 Sgr		24	7436	$0.64 \pm 0.38$	0.34	$9.1 \cdot 10^{-2}$
IX Vel		39	1264	$0.93 \pm 0.24$	0.54	$2.3 \cdot 10^{-4}$

While this inhibits the determination of actual colours of the flickering light sources, the difference of the scalegrams (on the logarithmic scale) obtained in different passbands will be constant as a function of time scale if the ratio of the flickering to the total light is the same on all time scales. If this is not observed the colour of flares on different time scales cannot be the same.

For all multicolour light curves the differences between the scalegrams in any passband and the  $B$ -band (which is taken as a reference) were calculated. Of course, only those time scales were regarded where the scalegrams are reliable. In Fig. 9 the scalegram differences of all light curves of V603 Aql and TT Ari, respectively, are plotted as examples. The broken lines are linear fits to the data. They are merely meant as a guide to visualize the trend. Although the scatter is quite large, one can see either a practically constant difference, or a slight decrease in “colours” with increasing time scale. This is confirmed by the other systems which are not shown in detail here.

This result indicates a general trend for shorter flickering flares to be at least on average somewhat bluer than the longer ones. In view of the large scatter of the data we refrain from further quantifying the correlation between colour and time scale.

### 5.3. Flickering properties as a function of CV type

According to their photometric behaviour CVs are classified into three major groups, namely novalike variables, classical and recurrent novae, and dwarf novae. Each of these groups is itself divided into more or less numerous subgroups. In a second dimension CVs can also be classified according to their magnetic behaviour into the major groups of non-magnetic systems (or systems where the magnetic fields are too weak to lead to easily observable effects), DQ Her systems (intermediate polars),

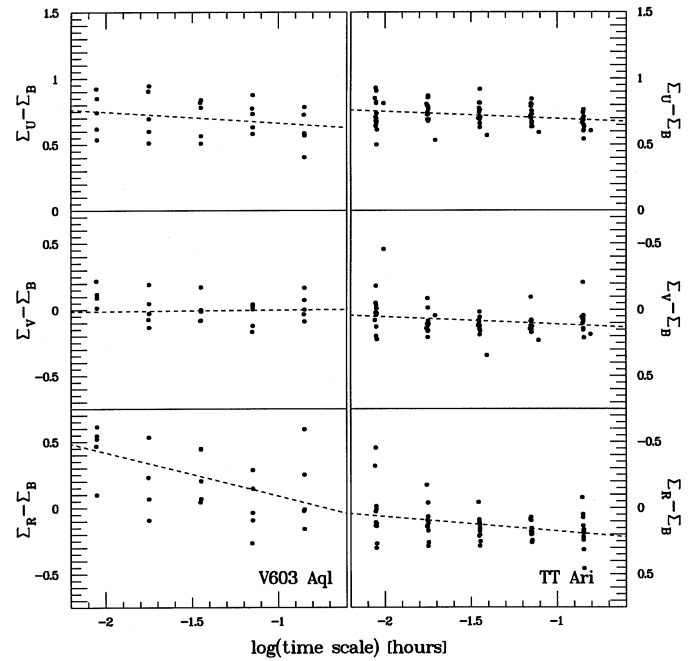


**Fig. 9.** Differences between the scalegram parameter  $\Sigma$  as measured in various bands of multicolour light curves and  $\Sigma$  in the reference band  $B$  for the systems V603 Aql and TT Ari. The slight decrease of all the differences indicates that flickering on shorter time scales is on average somewhat bluer than on longer time scales.

and AM Her stars (polars). For a detailed characterization of the photometric and magnetic classification, see e.g. the monograph of Warner (1995).

These groups and subgroups reflect the different physical conditions encountered in the respective systems, mainly the mass transfer between the components and the mass accretion rate onto the white dwarf, respectively, including their variation with time, and the strength of the magnetic field of the white dwarf. It is conceivable that these factors also influence the characteristics of the flickering: Flickering seems to be intimately related to the mass accretion process (Bruch 1992, 1995) which – involving plasma in the vicinity of a more or less magnetized body – is also likely to be influenced by magnetohydrodynamical processes. Therefore, the flickering properties of systems belonging to different groups are studied separately in order to look for systematic differences. Of considerable interest are the variations of the flickering properties around the outburst cycle of dwarf novae which will also be discussed.

#### 5.3.1. Novalike variables

Novalike systems as a whole occupy a broad range in the  $\alpha - \Sigma$ -plane, indicating very different relative contributions of the flickering to the total light and a widely scattered distribution among time scales. However, this becomes quite different, if the various subtypes are distinguished. In Fig. 10 the  $\alpha - \Sigma$ -plane for novalike variables is shown. Different subtypes occupy ranges with little or no overlap between each other, per-

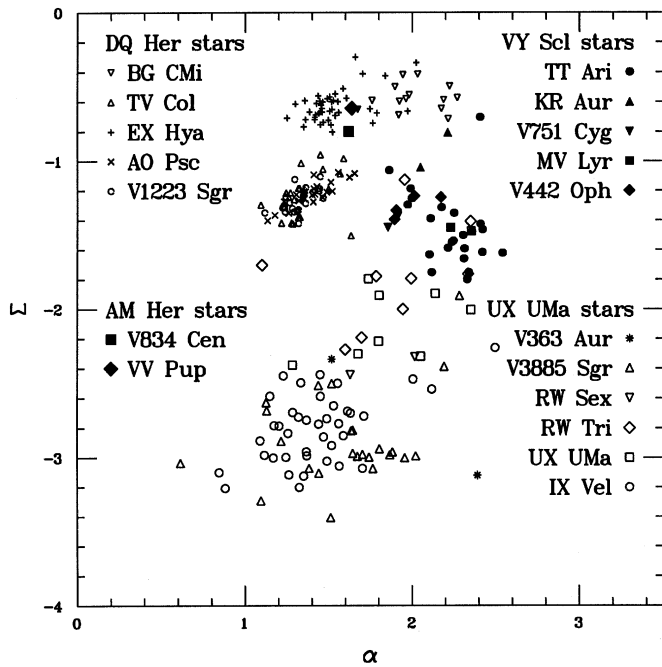


**Fig. 10.** Scalegram parameters  $\alpha$  and  $\Sigma$  for different subtypes of nova-like variables. The UX UMa stars, VY Scl stars and magnetic systems (intermediate polars and AM Her stars) are rather well separated from each other. In particular the magnetic systems are confined to two small distinct regions in the  $\alpha - \Sigma$ -plane, but it is not obvious which property determines this separation into two groups.

mitting a rather secure classification based only on their location in the  $\alpha - \Sigma$ -plane.

In the lower part of the diagram the UX UMa stars are grouped. These are the novalike variables which are always found in a comparatively stable high state.  $\Sigma$  being small reflects their well known low flickering amplitudes.  $\alpha$  is also on the mean fairly small, indicating that the dominance of slow flares over rapid ones is not strong. The distribution of the data points within the occupied region of the diagram is not uniform. However, this is due to a selection effect: The dense centre of the distribution is mainly caused by IX Vel of which many light curves are available. The extension of the distribution to the upper right is caused by RW Tri and UX UMa. The individual UX UMa stars are preferentially slightly separated from each other in the  $\alpha - \Sigma$ -plane, but there is still a considerable overlap.

The VY Scl stars are novalike variables which are normally found in a high state, but may drop occasionally for an unpredictable time into a several magnitudes fainter low state, presumably because of a reduced mass transfer rate from the secondary. Here, we regard only the high state, not enough light curves taken during low states being available. The present sample is dominated by a large number of light curves of TT Ari. The distribution in the  $\alpha - \Sigma$ -plane is clearly different from that of the UX UMa stars: The higher values of  $\Sigma$  indicate a much larger contribution of the flickering light source to the total light, the mostly larger value of  $\alpha$  shows, that the slow flares

dominate more strongly over the rapid ones. The overlap of the locations of different systems appears to be stronger than for the UX UMa stars, although the small number of lightcurves of some VY Scl stars demands caution concerning statistical conclusions.

The magnetic novalike variables of the DQ Her type again occupy a different and very distinct range in the  $\alpha - \Sigma$ -plane. They split up into two well separated subgroups, the lower one of which consists of TV Col, AO Psc and V1223 Sgr. The ranges of these three systems overlap completely. The upper subgroup consists of EX Hya<sup>8</sup> which forms the dense cluster at lower  $\alpha$  values but still overlaps considerably with BG CMi to which the majority of the points with higher  $\alpha$  belongs. The only two light curves of AM Her stars included in this study (referring to V834 Cen and VV Pup) also fall into this range. The high  $\Sigma$  values indicate the strong flickering contribution to the total light. Concerning the parameter  $\alpha$ , the DQ Her stars cannot be distinguished from the UX UMa stars but fairly well from the VY Scl stars. The most stunning feature is, however, the close confinement of TV Col, AO Psc and V1223 Sgr to a very narrow range in the  $\alpha - \Sigma$ -plane. It is not obvious what causes the clear separation between these stars on the one hand and EX Hya and BG CMi (and the polars) on the other hand.

The intriguing confinement of the magnetic systems to a narrow range (or better two quite similar ranges) as well as their clear separation from the other novalike variables (but note that dwarf novae in quiescence occupy a similar albeit broader range; see Sect. 5.3.3) suggests an origin of the flickering leading to properties which are distinct from those of non-magnetic CVs and at the same time similar to each other. Accretion onto magnetic white dwarfs does not occur via a boundary layer but via accretion columns or curtains. Accepting the view that flickering takes place primarily close to the white dwarf (Bruch 1992, 1996a), and that the accretion process itself leads to flickering, it is therefore not surprising that the flickering properties of magnetic and non-magnetic systems are different from each other. Whatever the source of the instability leading to flickering in magnetic systems is, it appears to be a much more “coherent” process than in the non-magnetic CVs.

### 5.3.2. Classical and recurrent novae

The classical novae fill the gap in the  $\alpha - \Sigma$ -plane between the different types of novalike variables (Fig. 11). Individual systems occupy preferred locations, reflecting the long-term stability discussed in Sect. 5.1, but their overlap is considerable. It is interesting to note that on average (but again with a certain overlap) fast novae have slightly larger values of  $\Sigma$  and smaller ones of  $\alpha$  than slow novae. Current nova outburst theories show that the speed of a nova, expressed e.g. through the  $t_2$ -time, depends

<sup>8</sup> EX Hya is sometimes regarded as a dwarf nova rather than a novalike variable because it occasionally (but rarely) exhibits a short lived, low amplitude eruption resembling to a certain degree a dwarf nova outburst. These brightenings being quite different from full fledged outbursts of dwarf novae of comparable orbital period, we prefer to regard EX Hya as a novalike variable here.

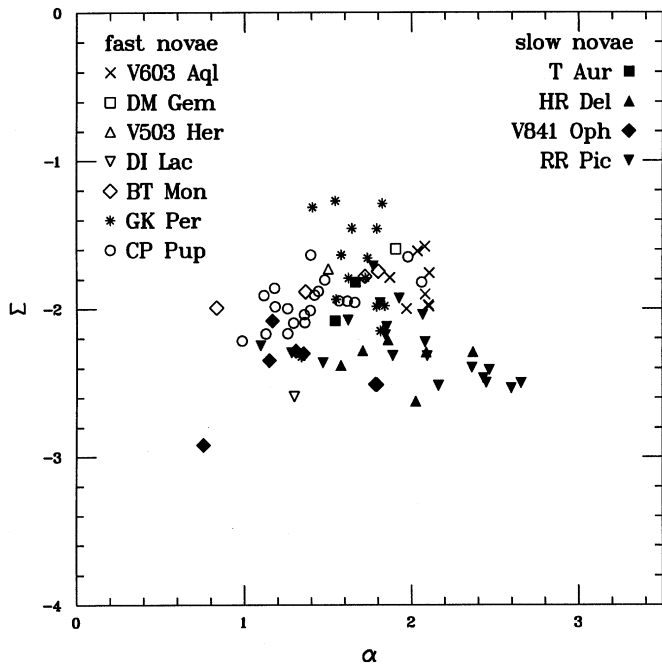


Fig. 11. Scalegram parameters  $\alpha$  and  $\Sigma$  for classical novae.

only on the primary mass and heavy element abundance of the accreted matter (Warner 1995). Assuming the latter to be constant for all systems, the faster novae are expected to have more massive primaries. Standard steady state accretion disk theory (probably not a bad approximation for old novae) predicts that they should also have hotter and more luminous accretion disks, provided other parameters such as mass transfer rate and disk radius are similar (Frank et al. 1985). If they nevertheless have larger values of  $\Sigma$ , and thus a stronger contribution of the flickering to the total light, this suggests that the flickering depends even stronger on the white dwarf mass than the disk luminosity (see also the discussion in Sect. 5.4).

For recurrent novae the statistics are very poor. Only three systems are available and at least for two of them (T CrB and RS Oph) the contribution of the secondaries is strong (and variable; see Bruch 1989), leading to considerable uncertainties in subtracting their light. This may contribute to a relatively wide distribution in  $\Sigma$  found for them. However,  $\alpha$  is not affected by this error source and remains within remarkable narrow limits, practically identical with the mean values of  $\alpha$  for classical novae.

### 5.3.3. Dwarf novae in quiescence and outburst

Dwarf novae are distinguished from other CVs by their more or less regular alternation between quiescent and outburst states. Details in their photometric behaviour justify the definition of subgroups: While the SS Cyg stars do not show major particularities, the Z Cam stars may get stuck for an unpredictable time in an intermediate state called standstill after an outburst. The SU UMa stars, apart from more numerous normal outbursts, exhibit from time to time a superoutburst with peculiar photomet-

ric properties. For an extensive characterization of the different subtypes see the reviews of e.g. la Dous (1994) and Warner (1995). Sometimes, the WZ Sge stars are considered as a separate group. They have rare, large amplitude outbursts which are indistinguishable from superoutbursts of SU UMa stars. Therefore, they are here regarded together with the latter group.

Concerning their flickering behaviour, as expressed by their location in the  $\alpha - \Sigma$ -plane shown in Figs. 12 – 15, the dwarf nova subtypes behave quite similarly. Slight differences exist, but the overlap is too large to assign a specific type to a system with any degree of certainty based on the  $\alpha - \Sigma$ -diagram alone. There is, however, a rather clear distinction between outburst and quiescent states, reflecting the fact that the amplitude of the flickering in dwarf novae (on a magnitude scale) is reduced during outbursts. While this was known for a long time (see e.g. Robinson 1973 for an early statement in this respect) a systematic study of this feature is here undertaken for the first time.

The results for the SS Cyg stars are summarized in Fig. 12. Concerning the outbursts only light curves sampled close to maximum light (as opposed to rise, decline or unknown outburst phases; see Table 1) were selected (the same holds true for the other dwarf nova types to be discussed below). Individual systems overlap considerably. Only few quiescent light curves are available. Their location in the  $\alpha - \Sigma$ -plane is clearly separated from the outburst light curves, the relative strength of the flickering being much stronger in quiescence. Although uncertain due to small-number statistics,  $\alpha$  appears to be much smaller in maximum than in quiescence for the prototypical system SS Cyg, indicating that rapid flares gain strength relative to slow ones in outbursts. This is in contrast to the general trend found in other dwarf novae (see Figs. 13 – 15).

The dichotomy between outburst and quiescence is much less conspicuous for the Z Cam stars (Fig. 13). There is even an overlap. These systems occupy a broader region in outburst than the SS Cyg stars but with the same centre. Again, the sample of quiescent light curves is small, making it difficult to decide if the observed smaller flickering contribution in Z Cam stars in quiescence is really significant. Flickering in the only light curve observed during a standstill appears to be better compatible with the quiescent state than with outbursts. This is surprising: It can be derived from the catalogue of Bruch & Engel (1994) that Z Cam stars in standstill are on the mean  $0^m.8 \pm 0^m.4$  fainter than in maximum and  $1^m.5 \pm 0^m.8$  brighter than in quiescence<sup>9</sup> and are thus closer to maximum than to minimum.

The sample of light curves of SU UMa stars is much larger than that of the other dwarf novae, permitting a more detailed comparison. Since many more observations during supermaximum are available than during normal maximum, we compare here the supermaximum state to quiescence. In order to avoid confusion in the  $\alpha - \Sigma$ -diagrams, the photometric states are separated into two diagrams: Fig. 14 refers to quiescence, Fig. 15 to supermaximum.

<sup>9</sup> The corresponding numbers for the star in question here, SY Cnc, are not known.

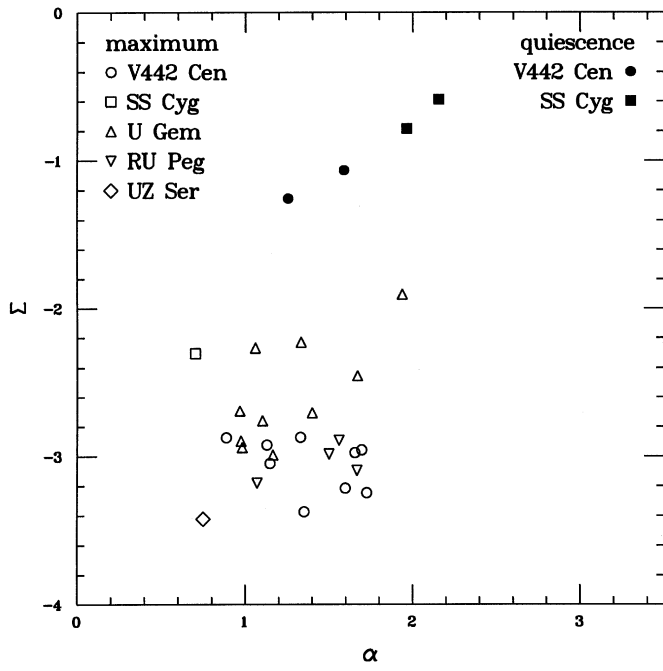


Fig. 12. Scalegram parameters  $\alpha$  and  $\Sigma$  for SS Cyg type dwarf novae in quiescence and outburst.

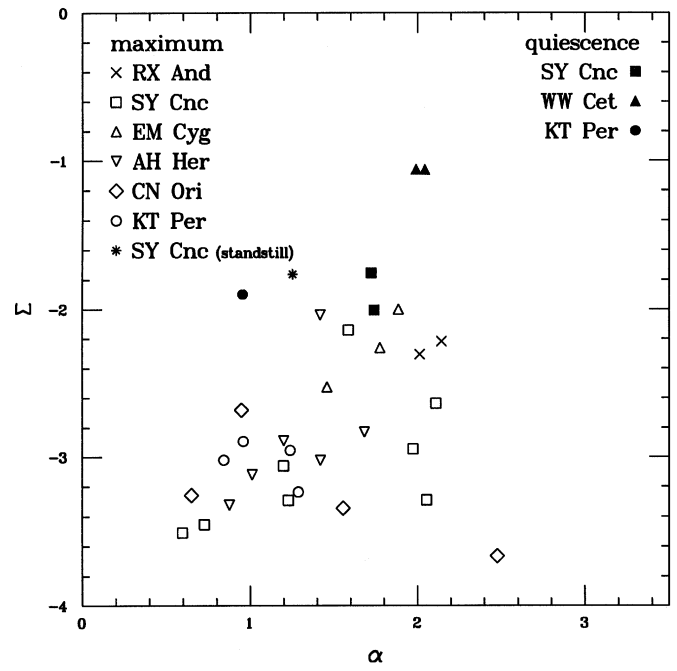


Fig. 13. Scalegram parameters  $\alpha$  and  $\Sigma$  for Z Cam type dwarf novae in various photometric states.

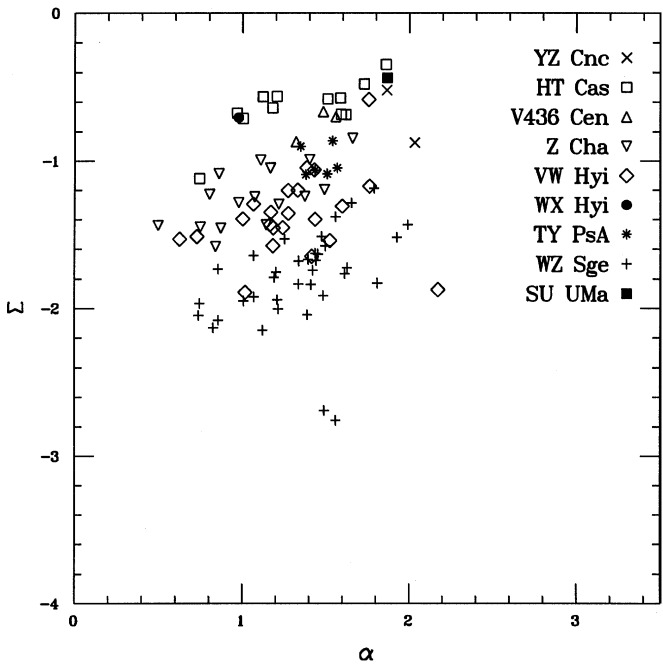


Fig. 14. Scalegram parameters  $\alpha$  and  $\Sigma$  for SU UMa type dwarf novae in quiescence.

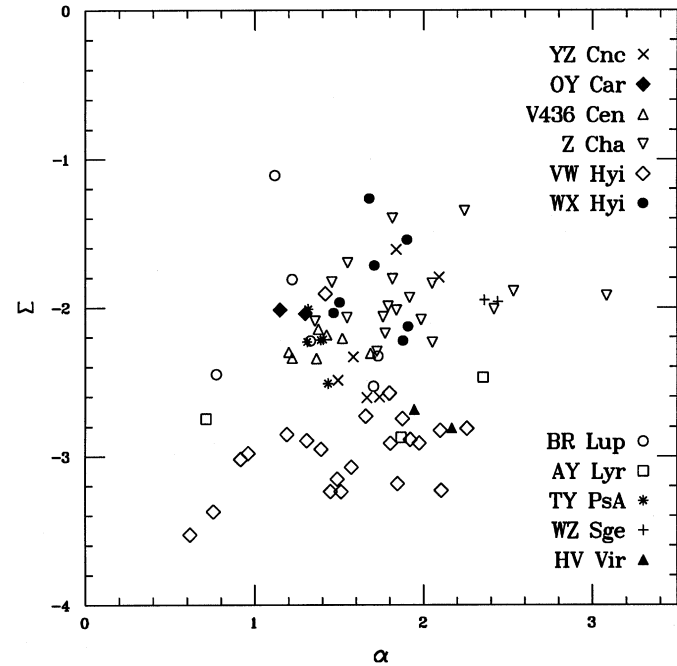


Fig. 15. Scalegram parameters  $\alpha$  and  $\Sigma$  for SU UMa type dwarf novae in superoutburst.

Compared to SS Cyg stars, the majority of the SU UMa stars show a stronger flickering during outburst. A notable exception is VW Hyi which populates a range well below most other systems in the  $\alpha - \Sigma$ -plane. The range of possible values of  $\alpha$  can be quite large even for an individual star. Except for a small overlap and disregarding WZ Sge for the moment, the quiescent light curves are well separated from those observed at supermaximum. As expected, the  $\Sigma$ -value is larger, and there is on the mean a small but significant shift towards smaller values of  $\alpha$ . Details of the behaviour are, however, dependent on the individual system. Regarding the stars with the largest statistical sample of light curves, Z Cha and VW Hyi, it is seen that whereas the mean value of  $\Sigma$  changes drastically and that of  $\alpha$  hardly from quiescence to outburst in VW Hyi, the opposite is true for Z Cha. A quite noticeable case is WZ Sge, which during quiescence straddles the borderline between outburst and quiescent states defined by the other SU UMa stars in both parameters,  $\alpha$  and  $\Sigma$ . During supermaximum, WZ Sge does not move in  $\Sigma$ , but  $\alpha$  increases significantly, i.e. flickering on longer time scales dominates more strongly than in quiescence (although the statistical sample is admittedly quite small).

The behaviour of the dwarf novae on the whole is thus rather heterogeneous in contrast to what was found for the novalike stars. It appears that dwarf novae are much more individualistic. This makes it difficult to draw immediate conclusions from their location in the  $\alpha - \Sigma$ -plane.

#### 5.3.4. Dwarf novae around the outburst cycle

For some dwarf novae a sufficiently large number of light curves taken in different photometric states (quiescence, outburst rise, maximum and decline) are available to study the behaviour of  $\Sigma$  and  $\alpha$  around the outburst cycle. For this purpose  $\Delta\Sigma = \Sigma - \Sigma_0$  as a function of  $\Delta m = m - m_0$  is regarded, where here and subsequently the index 0 stands for mean values observed in the quiescent state.

Since the data consist of non-calibrated white light curves, the magnitudes have to be taken from other sources. They were mostly interpolated in visual light curves published by members of the Variable Star Section of the Royal Astronomical Society of New Zealand (Bateson 1977a,b,c, 1979, Bateson & Dodson 1984, Bateson & McIntosh 1985, 1986a,b). For WZ Sge the corresponding information was extracted from Fig. 1 of Patterson et al. (1981). Obviously, the errors associated with these magnitudes are quite large, amounting easily to 0<sup>m</sup>.5.

$\Delta\Sigma$  is plotted as a function of  $\Delta m$  in Fig. 16 for six systems with ten or more available light curves (WZ Sge has been omitted; it has already been shown in Sect. 5.3.3 that  $\Sigma$  does not change systematically between quiescence and outburst).

According to the definition of the normalized scalegram in Sect. 4.3,

$$\begin{aligned} \Delta\Sigma &= \log \left( \frac{S'}{S'_0} \frac{N \Delta t}{N_0 (\Delta t)_0} \frac{\sum_{i=1}^{N_0} x_{0,i}^2}{\sum_{i=1}^N x_i^2} \right) \\ &\approx \log \left( \frac{S'}{S'_0} \frac{N \Delta t}{N_0 (\Delta t)_0} \frac{\bar{x}_0^2}{\bar{x}^2} \right) \end{aligned} \quad (9)$$

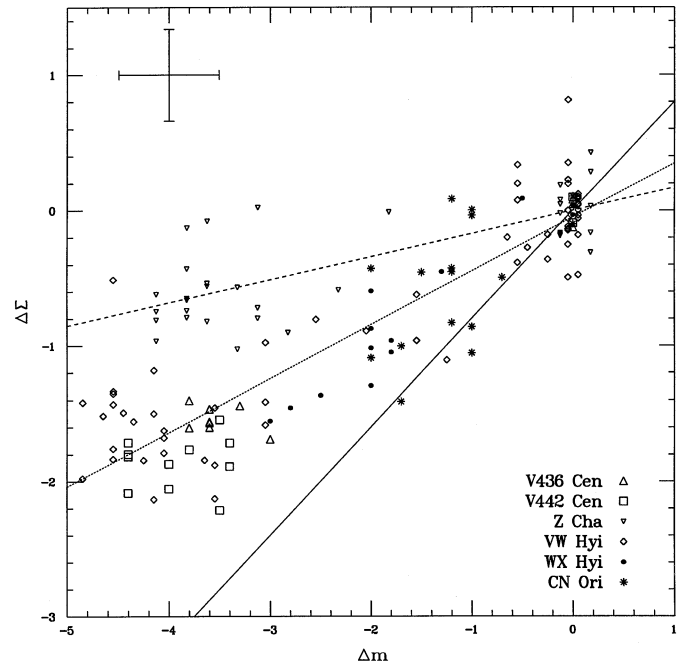


**Fig. 16.** Difference  $\Delta\Sigma$  between the mean value of the scalegram parameter  $\Sigma$  during quiescence and the observed value in a particular light curve as a function of the difference  $\Delta m$  between the mean quiescent magnitude and the magnitude at the time of the observations for light curves of 6 dwarf novae around the outburst cycle. The solid line indicates the expected relation between  $\Delta m$  and  $\Delta\Sigma$  in the case that the intrinsic flickering strength does not change as the system brightens. The data remaining above this line means that the intrinsic flickering strength rises during outbursts, but not as much as the total light. The dashed and dotted lines represent linear least squares fits to the data points of Z Cha and to all other data, respectively. The latter behave remarkably similar to each other. A typical error bar is shown in the upper left corner.

where  $N$  is the number of data points in the light curve and  $x$  is the signal (e.g. count rate). The approximation in the second line is valid if the flickering signal is not too strong. Under the assumption that the flickering strength does not change intrinsically during the outburst cycle,  $S^* \equiv S' N \Delta t = S'_0 N_0 (\Delta t)_0 \equiv S_0^*$ . Considering Pogson's equation, this yields the simple relation

$$\Delta\Sigma = a \Delta m \quad (10)$$

with  $a = 0.8$ . It is shown in Fig. 16 as a solid line. Tests with artificial light curves confirm the prediction excellently. If in contrast the flickering light source would increase to the same degree as the background light  $\Sigma$  would obviously not change during the outburst cycle.

The observed data form a sequence well above the solid line but are far from constant, reflecting the intrinsic increase of flickering during an outburst which, however, remains smaller than the brightening of the system as a whole. But more surprising is the fact that – with the noticeable exception of Z Cha – all systems follow the same relation. A least squares fit to all points (excluding Z Cha) yields the dotted line in the Fig. 16

which has an inclination of  $a = 0.40 \pm 0.01$ . The corresponding number for Z Cha (broken line) is  $a = 0.17 \pm 0.02$ .

Substituting Eq. (9) on the left hand side of Eq. (10) and using Pogson's equation on the right side, it is verified that

$$\frac{S^*}{S_0^*} = \left( \frac{\bar{x}}{\bar{x}_0} \right)^{-2.5a+2} \quad (11)$$

With  $a = 0.40$  this gives  $S^*/S_0^* = \bar{x}/\bar{x}_0$ . Remembering that  $S^*$  is basically the energy of the variable signal on a given scale,  $\sqrt{S^*}$  can be regarded as proportional to the amplitude of the flickering in the light curve. Thus, during the outburst cycle the intrinsic flickering amplitude changes as the square root of the mean light of the system. However, the exceptional case of Z Cha, where we get  $S^*/S_0^* = (\bar{x}/\bar{x}_0)^{1.6}$ , reminds us that this simple relation may well be a coincidence rather than reflecting an equally simple fundamental physical principle behind the flickering!

The dependence of  $\Delta\alpha$  on  $\Delta m$  is not as well defined as that of  $\Delta\Sigma$ . In Fig. 17 the relation is shown for Z Cha, VW Hyi and WZ Sge. In all other investigated cases, no clear dependence was found. In spite of the large scatter, a systematic increase of  $\alpha$  is found as the system brightens, starting, however, only well above the quiescent level. Moreover, the degree of increase is not the same for the three systems.

An increase of  $\alpha$  means that flickering on small time scales is reduced relative to that on long scales. In his study of the location of the flickering light source in Z Cha, Bruch (1996a) has shown that on time scales below one minute at least two sources contribute: a region close to the white dwarf and the hot spot. During outburst, hot spot flickering disappears. Assuming it to occur predominantly on short time scales, its disappearance in bright states may cause the shift towards larger  $\alpha$ -values observed in the three mentioned systems. Note that all of them exhibit a well developed orbital hump as a clear sign of a strong contribution of the hot spot to the total light. This is not the case in those systems where  $\Delta\alpha$  is independent of  $\Delta m$ .

The above results might be subject to an error if the exact shape of the scalegram and thus the residuals of the linear fit differ systematically through the outburst cycle. This could cause systematic modifications of  $\Sigma$  and  $\alpha$ . The residuals were therefore checked carefully for such an effect. In no case were significant differences detected in their behaviour during quiescence and outburst. Another systematic error might occur because dwarf novae are known to undergo appreciable colour changes during the outburst (see e.g. Bailey 1980), causing a modification of the effective wavelength of the bandpass of the white light curves. This effect may also cause changes of  $\Sigma$  and  $\alpha$ . However, since the discussed trends in Figs. 16 and 17 remain visible in spite of the large accidental errors of  $\Delta\Sigma$  and  $\Delta\alpha$  as well as of  $\Delta m$  we presume that his error source is not large enough to invalidate the above findings.

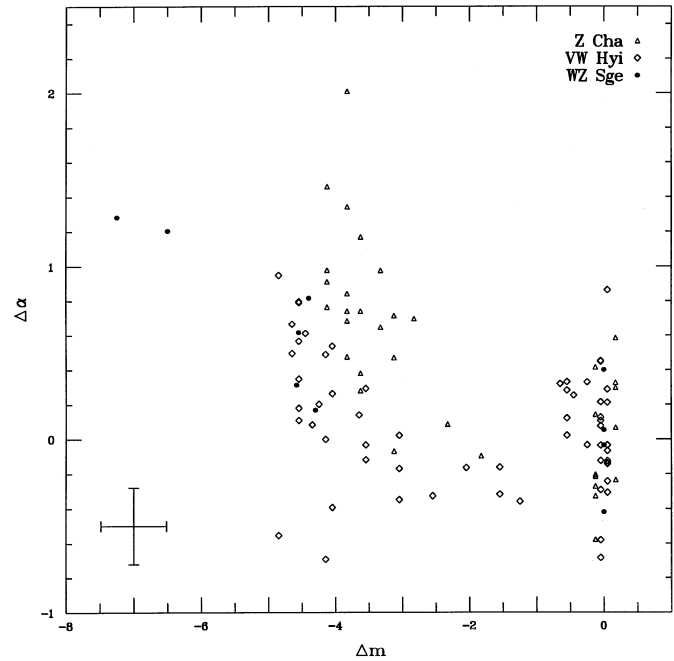


**Fig. 17.** Difference  $\Delta\alpha$  between the mean value of the scalegram parameter  $\alpha$  during quiescence and the observed value in a particular light curve as a function of the difference  $\Delta m$  between the mean quiescent magnitude and the magnitude at the time of the observations for light curves of 3 dwarf novae with a strong orbital hump. A tendency for an increase of  $\Delta\alpha$  with increasing system brightness is seen, indicating a steepening of the scalegram and thus a reduced flickering strength on small time scales during outbursts. A typical error bar is shown in the lower left corner.

#### 5.4. Correlations with dynamical and geometrical system parameters

It has been notoriously difficult to find convincing correlations between properties of the flickering and dynamical (such as masses or periods) or geometrical (such as dimensions or inclinations) parameters of the cataclysmic binaries (Bruch 1989, 1992; Beckemper 1995; Nohlen 1995; Sand 1994).

Bruch (1992) has argued that the major part of the flickering can only arise in the immediate vicinity of the white dwarf – the inner accretion disk, the boundary layer or on the white dwarf itself – since only here enough energy is available to power the considerable luminosity of the flickering light source. Later, Bruch (1996a) has shown that in the particular system Z Cha flickering comes indeed mainly from a region very close to the white dwarf (with a smaller contribution from the hot spot seen only during quiescence). Similar results were also found for other systems (see Sect. 1). One might therefore expect a correlation with the white dwarf mass: The more massive it is, the more gravitational energy can be released and the stronger will be the flickering. However, the luminosity of the accretion disk also increases with the mass of the central star. Since most of our light curves are not calibrated and we can therefore only measure the strength of the flickering relative to the background light (i.e. basically the unmodulated light of the accretion disk)

the mass dependence will cancel out (at least in a first order approximation if flickering strength and disk brightness scale in the same way with the white dwarf mass in the observed wavelength band). Any empirical search for a correlation between the strength of the flickering and the white dwarf mass will also be hampered because the latter is normally known only with a considerable uncertainty in CVs.

Accepting the picture that flickering is due to a turbulent mass flow in the inner disk or an unsteady dumping of mass onto the white dwarf, the situation becomes even more complicated considering that the flickering strength is then expected to depend also on the mass accretion rate. Numerical values of this quantity are highly uncertain and (at least in dwarf novae) can differ strongly from the rate at which mass is transferred from the secondary, depending on the photometric state. A higher mass accretion rate will lead to an increased luminosity of the flickering light source, but individual flares may also be expected to overlap stronger, leading to a decrease of the degree of modulation and thus of observable flickering activity. This is in line with the finding in Sect. 5.3.4 that the flickering increases less than the total light in dwarf nova outbursts.

A further complication is a possible dependence of relative flickering strength on the orbital inclination. In fact, Bruch (1992) and Sand (1994) found some indications for such a correlation but not yet convincing evidence. This could come about if the flickering light source and the accretion disk are not coplanar, leading to different foreshortening factors if viewed under different inclinations. Such a situation can be realized if the site of the flickering is a boundary layer not restricted to a narrow equatorial belt but engulfing a larger part of the white dwarf (Livio & Truran 1990).

We thus face the situation where the luminosity of the flickering light source, its contribution relative to the background light, and its modulation must be expected to depend in an unknown way on parameters such as the white dwarf mass, the (time dependent) accretion rate, and the orbital inclination, all of which are in most cases not well known. Lacking a physical model for the flickering, and being only able to measure parameters of the flickering which are related via possibly complicated functions to the basic properties of the underlying light source, which itself depends (probably) on more fundamental system parameters, one cannot expect simple relationships between observable flickering characteristics and dynamical or geometrical properties of individual CVs to exist.

In an attempt to nevertheless find significant correlations we plot in Fig. 18 the mean values of the parameter  $\Sigma$  for individual systems as a function of the white dwarf mass. Only light curves corresponding to an accretion disk in the bright state (i.e. classical novae, novalike variables in the high state and dwarf novae in outburst) are considered. The disks being in quite a different state in quiescent dwarf novae, these should not be compared to novae and novalikes. Moreover, magnetic systems are excluded since they have a truncated accretion disk or even none at all, and the mechanism leading to flickering might therefore not be identical to that in non-magnetic CVs (see the discussion in Sect. 5.3.1). The figure does not show a strict correlation [for-

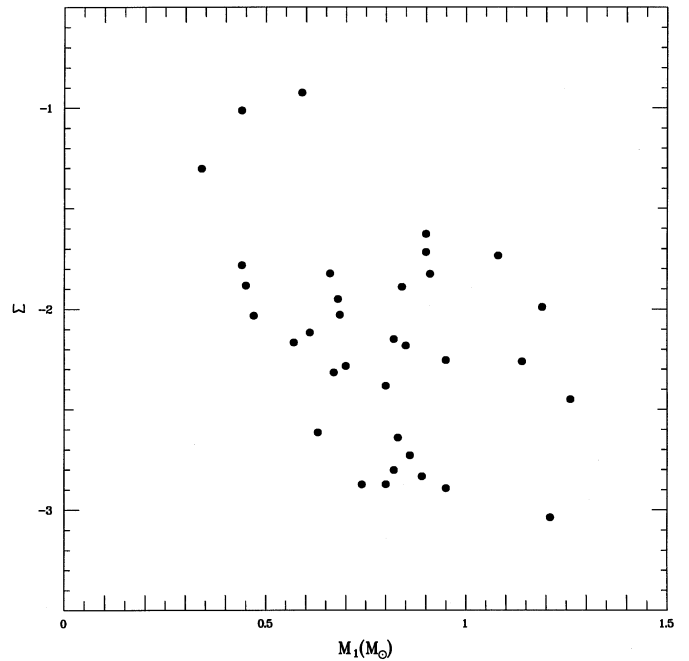


**Fig. 18.** Mean value of the scalegram parameter  $\Sigma$  for individual systems with accretions disks in the bright state as a function of the white dwarf mass. No clear correlation exists, but a significant trend is obvious.

mal statistics yield a correlation coefficient of  $-0.43$  and a “false alarm” probability (see Sect. 5.1) of  $7.5 \times 10^{-3}$ ] but exhibits a clear trend which is opposite to what is naively expected: The flickering strength is on the mean reduced in systems with a higher white dwarf mass. Within the above argumentation this means that either the background light increases quicker than the flickering with the white dwarf mass, or the modulation of the flickering light source is lower in more massive systems.

It is not sensible to quantify the dependence of  $\Sigma$  on the mass accretion rate because of the large observational uncertainties of the latter. In principal the mass transfer rate could be estimated using the absolute magnitudes of the CVs. However, this would require knowledge of the distance (in most cases only known with a large error margin), an uncertain correction for the orbital inclination and an equally uncertain bolometric correction. It is known that a rough dependence of mass transfer rate on orbital period  $P$  exists (e.g. Patterson 1984). Thus, any correlation of  $\Sigma$  with  $P$  may indicate a correlation with  $\dot{M}$ . For the same sample<sup>10</sup> as above, Fig. 19 shows  $\Sigma$  as a function of  $P$  (inclusion of the magnetic systems does not alter the general properties of the diagram). Again, no clear correlation exists, but there seems to be an upper limit which decreases with increasing  $P$  and which is qualitatively consistent with the idea of a decreasing degree of modulation of the flickering light source with orbital period and thus mass transfer rate. However, since such a relation is only suggested as an upper limit there must be other components able to diminish the flickering strength. We

<sup>10</sup> Two systems, BV Cen and GK Per are beyond the upper period limit of Fig. 19.

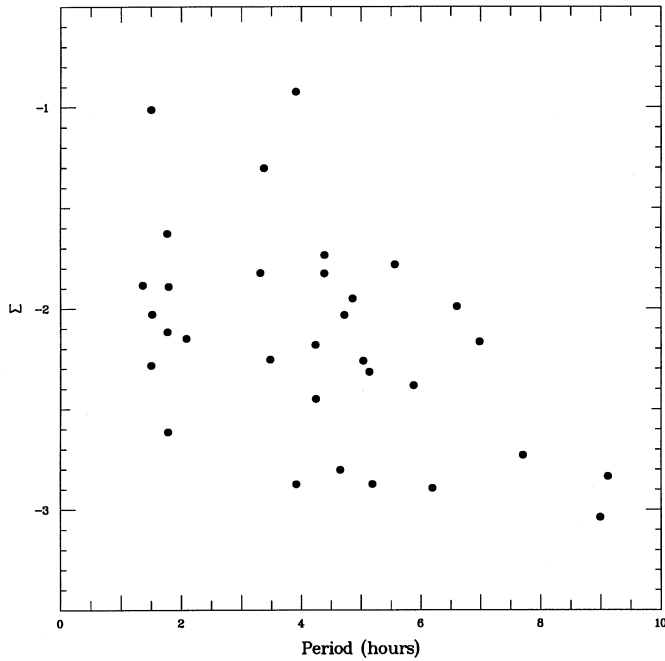


**Fig. 19.** Mean value of the scalegram parameter  $\Sigma$  for individual systems with accretion disks in the bright state as a function of the orbital period. No correlation exists, but there appears to be an upper boundary line which is consistent with the idea of a decreasing degree of modulation of the flickering light source with increasing period and thus mass accretion rate.

tested if the orbital inclination can be responsible but did not find a correlation.

Even more elusive concerning correlations with dynamical and geometrical system parameters than the flickering strength  $\Sigma$  is the inclination  $\alpha$  of the scalegrams. We found no case where a correlation or even a significant trend was visible which could teach us something about the physical nature of the flickering.

## 6. Conclusions

We applied the recently developed technique of wavelet transforms for the first time to light curves of cataclysmic variables in order to quantify statistical properties of the stochastic variations known as flickering in these systems. Since we plough virgin lands we first discuss in some detail the requirement a light curve has to fulfill to be suitable for such an analysis, the choice of the optimal wavelet, error estimates via bootstrap replications, normalization, and the influence of various sources of noise in the data.

The scalegram is chosen as an appropriate tool to quantify the strength of the flickering as a function of time scale. On a double logarithmic scale the scalegram is always found to be linear over the entire range of time scales over which statistically reliable wavelet coefficients can be measured, indicating that flickering is a self-similar process over several decades. This simple behaviour of the scalegram enables the introduction of two parameters, the inclination  $\alpha$  of the scalegram and the flick-

ering strength  $\Sigma$  at a reference time scale of  $3^m$ .  $\alpha$  and  $\Sigma$  contain the relevant information concerning the WT of flickering light curves almost completely.

A total of 776 light curves of 73 CVs in different photometric states were subjected to a WT. This large number enables a search for meaningful differences and common properties of flickering in different CV subtypes.

We find that on long time scales (up to 20 years) flickering is a stable process as indicated by the stability of the scalegram parameters  $\alpha$  and  $\Sigma$ . However, on short time scales variations occur which are more evident for  $\alpha$  than for  $\Sigma$  (possibly due to the smaller errors of  $\alpha$ ). There is a tendency for a positive correlation between  $\alpha$  and  $\Sigma$  (albeit with some remarkable exceptions), indicating that as the flickering gets stronger (relative to the background light!) the scalegram becomes steeper, reflecting a stronger dominance of slow flickering flares over rapid ones.

Concerning the colours of the flickering, the analysis of multicolour light curves reveals a tendency for shorter flares to be on average somewhat bluer than longer ones.

Different types of CVs are found to populate different regimes in the  $\alpha - \Sigma$ -plane. This behaviour is particularly clear cut for novalike variables: The UX UMa type systems hardly overlap with the VY Scl stars which have systematically lower values of  $\alpha$  and  $\Sigma$ . The magnetic CVs – intermediate polars as well as AM Her stars – cluster in a remarkably small region of the  $\alpha - \Sigma$ -plane – distinct from both, UX UMa stars and VY Scl stars – and are themselves split into two groups (although it is not clear what causes the latter distinction). For novae and dwarf novae there are some tendencies concerning their location in the  $\alpha - \Sigma$ -plane but not such sharp differences as for the novalike variables. Of course, differences between outburst and quiescent states of dwarf novae exist.

The data base permits us to investigate systematical changes of  $\alpha$  and  $\Sigma$  through the outburst cycles of several dwarf novae. For the first time we quantify the evolution of the flickering strength as a function of the brightness above quiescence: For all investigated systems (with the noticeable exception of Z Cha) the intrinsic flickering amplitude scales with the square root of the mean light of the system. In those dwarf novae where the hot spot causes a strong hump in the quiescent light curves  $\alpha$  increases during the outburst, revealing a relative reduction of flickering on short time scales.

Flickering must be regarded as the observable consequence of some instabilities in CVs, related in a complicated, non-linear way to the driving mechanisms which may themselves be related to other observable system parameters in a no less complicated way. This explains why clear cut correlations of the flickering characteristics with dynamical and/or geometrical properties of the CVs are so hard to find in general and were not found here. At most some trends are visible.

The results of this study define boundary conditions for models of the flickering. To date, no real physical model exists. Statistical (shot noise) models were formulated for polars by Panek (1980) and Larsson & Larsson (1995), but not for non-magnetic CVs or DQ Her stars. While such models cannot

substitute a physical one if one wants to understand the origins of flickering, it is “one step closer” to a physical model than mere quantification of the observable properties of flickering. The next obvious step to undertake is thus the attempt to investigate (1) if a shot noise model can reproduce light curves with properties as found in this study, and (2) what must be the properties of such shots (frequency, strength, shape) to lead to scalegram parameters as observed for the different types of CVs and photometric states.

*Acknowledgements.* We are very much indebted to the numerous colleagues who have put their light curves at our disposal. Above all we thank D. O’Donoghue and B. Warner (Cape Town) and N.E. Nather, R.E. Robinson and E.-H. Zhang (Austin) who gave us access to their vast light curve archives. Further data we got from R. Baptista, N.G. Beskrovnaya, L. Chiappetti, V.P. Goranskij, C. Hellier, A. Hollander, J. Kałużny, M. Kubiak, I. Semeniuk, S. Shugarov, C. Sterken, K. Reinsch and S. Rößiger. Without their help this work could not have been done. It was also supported by a travel grant of the Deutsche Forschungsgemeinschaft.

## References

- Bailey J., 1980, MNRAS 190, 119  
 Bateson F.M., 1977a, New Zealand Journ. of Science 20, 73  
 Bateson F.M., 1977b, Publ. V.S.S., RASNZ, 5, 10  
 Bateson F.M., 1977c, Publ. V.S.S., RASNZ, 5, 27  
 Bateson F.M., 1979, Publ. V.S.S., RASNZ, 7, 29  
 Bateson F.M., Dodson A.W., 1984, Publ. V.S.S., RASNZ, 12, 69  
 Bateson F.M., McIntosh R., 1985, Publ. V.S.S., RASNZ, 13, 1  
 Bateson F.M., McIntosh R., 1986a, Publ. V.S.S., RASNZ, 14, 1  
 Bateson F.M., McIntosh R., 1986b, Publ. V.S.S., RASNZ, 14, 67  
 Beckemper S., 1995, *Statistische Untersuchungen zur Stärke des Flickering in kataklysmischen Veränderlichen*, diploma thesis, Münster  
 Beskrovnaya N.G., Ikhsanov N.R., Bruch A., Shakhovskoy N.M., 1996, A&A 307, 840  
 Bortle J., 1985, IAU Circ. 4077  
 Bruch A., 1989, *Eigenschaften und Ursachen des Flickering in kataklysmischen Veränderlichen*, habil. thesis, Münster  
 Bruch A., 1991, A&A 251, 59  
 Bruch A., 1992, A&A 266, 237  
 Bruch A., 1995, in: J. Greiner et al. (eds.) *Flares and Flashes*, Proc. IAU Coll. 151, p. 288  
 Bruch A., 1996a, A&A 312, 97  
 Bruch A., 1996b, in: A. Evans, J.H. Wood (eds.): *Cataclysmic Variables and Related Objects*, Proc. IAU Coll. 158, Astrophys. Sp. Sc. Lib. Vol. 208, Kluwer, Dordrecht, p. 35  
 Bruch A., Engel A., 1994, A&AS 104, 79  
 Bruch A., Grütter M., 1997, Acta Astron. 47, 307  
 Chui C.K., 1992, *An Introduction to Wavelets*, Academic Press Inc., San Diego  
 Coifman R., Wickerhauser M.V., 1992, IEEE Trans. on Information Theory, 38, 719  
 Daubechies I., 1992, *Ten lectures on wavelets*, CBMS–NSF Series in Applied Mathematics, Vol. 61, SIAM Publications, Philadelphia  
 Diaz M.P., Steiner J.E., 1995, AJ 110, 1816  
 Donoho D.L., 1992, Technical Report 416, Department of Statistics, Stanford University  
 Donoho D.L., Johnstone I.M., 1993, Technical Report 425, Department of Statistics, Stanford University  
 Efron B., Tibshirani R.J., 1993, *An Introduction to the Bootstrap*, Chapman & Hall, London  
 Elsworth Y., James J.F., 1986, MNRAS 220, 895  
 Frank J., King A.R., Raine D.J., 1985, *Accretion Power in Astrophysics*, Cambridge University Press, Cambridge  
 Horne K., Stiening R.F., 1985, MNRAS 216, 933  
 Horne K., Marsh T.R., Cheng F.H., Hubeny I., Lanz T., 1994, ApJ 426, 294  
 Jawerth B., Sweldens W., 1993, *An Overview of Wavelet Based Multiresolution Analysis*, Dep. of Mathematics, Univ. South Carolina, *SIAM Review*  
 la Dous C., 1994, SSR 67, 1  
 Larsson S., Larsson B., 1995, in: J. Greiner et al. (eds.) *Flares and Flashes*, Proc. IAU Coll. 151, p. 296  
 Livio M., Truran J.W., 1990, Comm. Astrophys. 14, 221  
 Mallat S., 1989, Trans. Amer. Math. Soc. 315, 69  
 Nohlen C., 1995, *Das Frequenzverhalten des Flickering von kataklysmischen Veränderlichen*, diploma thesis, Münster  
 Panek R.J., 1980, ApJ 241, 1077  
 Patterson J., 1984, ApJS 54, 443  
 Patterson J., McGraw J.T., Coleman L., Africano, J.L., 1981, ApJ 248, 1067  
 Press W.H., Flannery B.P., Teukolsky S.A., Vetterling E.L., 1980, *Numerical Recipes in C*, Cambridge University Press, Cambridge  
 Robinson E.L., 1973, ApJ 183, 193  
 Sand M., 1994, *Untersuchung statistischer Parameter des Flickerings von kataklysmischen Veränderlichen*, diploma thesis, Münster  
 Scargle J.D., Steinman-Cameron T.Y., Young K., Donoho D.L., Crutchfield J.P., Imamura J., 1993, ApJ 411, L91  
 Steiman-Cameron T.Y., Young K., Scargle J.D., Crutchfield J.P., Imamura J., Wolff M.T., Wood K.S., 1994, ApJ 435, 775  
 van Paradijs J., Kraakman H., van Amerongen S., 1989, A&AS 79, 205  
 Verdenet M., 1984, IAU Circ. 3907  
 Verdenet M., 1985, IAU Circ. 4077  
 Warner B., 1995, *Cataclysmic Variable Stars*, Cambridge University Press, Cambridge  
 Warner B., Nather R.E., 1971, MNRAS 152, 219  
 Welsh W.F., Wood J.H., 1995, in: J. Greiner et al. (eds.) *Flares and Flashes*, Proc. IAU Coll. 151, p. 300  
 Welsh W.F., Wood J.H., Horne K., 1996, in: A. Evans, J.H. Wood (eds.): *Cataclysmic Variables and Related Objects*, Proc. IAU Coll. 158, Astrophys. Sp. Sc. Lib. Vol. 208, Kluwer, Dordrecht, p. 29